International Atomic Energy Agency

INDC(CCP)-399
Distr.: L

INDC INTERNATIONAL NUCLEAR DATA COMMITTEE

SELECTED ARTICLES TRANSLATED FROM JADERNYE KONSTANTY (NUCLEAR CONSTANTS) VOLUME 2, 1993 AND VOLUMES 1 AND 2, 1994

Translated by the IAEA

December 1995

IAEA NUCLEAR DATA SECTION, WAGRAMERSTRASSE 5, A-1400 VIENNA

Reproduced by the IAEA in Austria
December 1995

INDC(CCP)-399
Distr.: L

SELECTED ARTICLES TRANSLATED FROM JADERNYE KONSTANTY (NUCLEAR CONSTANTS) VOLUME 2, 1993 AND VOLUMES 1 AND 2, 1994

Translated by the IAEA

December 1995

CONTENTS

95-10765 (G)
Translated from Russian

UDC 539.172.3

CROSS-SECTIONS FOR THE $^{63,65,nat}Cu(\gamma,np)$ REACTIONS IN THE GIANT DIPOLE RESONANCE REGION

V.V. Varlamov, N.G. Efimkin, B.S. Ishkhanov, V.V. Sapunenko and M.E. Stepanov

Scientific Research Institute for Nuclear Physics
Moscow State University, Moscow

ABSTRACT

The published data on a number of photonuclear reaction cross-sections for $^{63,65,nat}Cu$ have been compared and the conditions under which they were obtained analysed in detail. In order to eliminate the existing discrepancies between the results of the various studies, the authors have proposed a new procedure for normalization of the initial data by the difference method of determination of the $^{63}Cu(\gamma,np)$ reaction cross-section and a new procedure for their energy calibration. The data obtained for this reaction have also been used to evaluate new data for the $^{65,nat}Cu(\gamma,np)$ reactions.

INTRODUCTION

Accurate and reliable information on cross-sections for the various photonuclear reactions with copper nuclei is of great interest in both basic and applied nuclear physics research.

The photonuclear reactions for these nuclei are highly convenient for verifying the predictions of theoretical calculations based on various model representations of the processes of photon-induced decay of nuclei in this region. Moreover, owing to a number of physical and chemical properties of copper targets, the reaction cross-sections for such targets have become widely accepted as standards in photonuclear experiments, with respect to which not only absolute normalization of the results of relative measurements is performed but also experimental methods are calibrated.

Of the greatest interest are the cross-sections for the main photon-induced decay channels - the single-nucleon reactions (γ,n) and (γ,p). However, the specific characteristics of the majority of the traditionally most common methods of direct recording of product particles in photonuclear experiments to study these reactions are such that it is only possible to obtain information on the sum of the reactions: [(γ,n) + (γ,np)] and [(γ,p) + (γ,np)], respectively. In this connection, an additional source for improving the accuracy and reliability of data on photoproton and photoneutron reactions is the data on the (γ,np) reaction, since they serve as a kind of connecting link between the results for these two main photon-induced decay channels.

While it is possible in principle to make a direct measurement of the (γ,np) reaction cross-section for other target nuclei by the activation method, this is either impossible or inefficient in the case of the copper isotopes ^{63,65}Cu, because the residual nuclei are either the stable isotope ^{61}Ni or the isotope ^{63}Ni, which has a half-life of about 100 years.

It is of sufficient topical interest, therefore, to obtain reliable and accurate data on cross-sections for the ^{63,65,nat}Cu(γ,np) reactions by analysing the available experimental material. The aim of this paper is to resolve this problem on the basis of a combined analysis of mutually complementary data on the photonuclear reaction cross-sections for the two copper isotopes and their natural mixture (information on the abundances of the copper isotopes and the thresholds for some reactions which are of the greatest importance for subsequent discussion is given in Table 1).

TABLE 1. ABUNDANCES OF THE COPPER ISOTOPES AND THRESHOLDS OF SOME REACTIONS

Isotope	Distribution (%)	Particle separation energy in reactions, MeV				
		γ,n	γ,p	γ,np	γ,2n	γ,2p
^{63}Cu	69.17	10.9	6.1	16.7	19.7	17.2
^{65}Cu	30.83	9.9	7.4	17.1	17.8	20.0

EXPERIMENTAL DATA

To date, results have been published for only two experiments on the determination of the cross-section for the (γ,np) reaction with copper nuclei - measurements for a target consisting of a natural mixture of copper isotopes [1] and for the ^{63}Cu nucleus [2].

In Ref. [1] the yield curve for the ^{nat}Cu(γ,np) reaction was obtained by subtracting from the yield curve for the total (γ,Xn) photoneutron reaction the yield curve for the sum of the reactions ^{63}Cu((γ,n) + 2(γ,2n)), published earlier [3], normalized on the assumption that the cross-section of the various photonuclear reactions for the two copper isotopes are proportional to one another (which, broadly speaking, is not quite obvious). The photon difference method [4] typical of the 1950s and 1960s was used with a calculation step of 2 MeV in order to derive the energy dependence of the cross-section from the yield curve so obtained. Figure 1 shows the cross-section for ^{nat}Cu(γ,np) given in Ref. [1] and the cross-section for ^{63}Cu(γ,np) which we recalculated from it, taking into account the isotopic abundance in the natural mixture and assuming the same doubtful similarity of the cross-sections for both isotopes. Together with these, Fig. 1 also shows the cross-section for ^{63}Cu(γ,np) from Ref. [2].

In Ref. [2] the cross-section for $^{63}Cu(\gamma,np)$ was obtained by subtracting the cross-section for $^{63}Cu(\gamma,n)$ determined by the activation method from the cross-section for $^{63}Cu((\gamma,n) + (\gamma,np))$ obtained in Ref. [5] using a beam of quasi-monoenergetic annihilation photons and the direct method of measuring photoneutron multiplicity. Both are given in Fig. 2. The two cross-sections were normalized on the basis of the data in the energy region below the threshold of the $^{63}Cu(\gamma,np)$ reaction - E_{thresh} = 16.7 MeV. The $^{63}Cu(\gamma,np)$ reaction cross-section thus obtained is given in Fig. 1.

Comparison of the data in Fig. 1 shows that they differ substantially from each other both in magnitude and shape. It should also be noted that they are both open to serious criticism, since they are in poor agreement with other cross-sections, in particular those for the $(\gamma,n) + (\gamma,np)$ and $(\gamma,p) + (\gamma,np)$ reactions.

Firstly, the cross-section for $^{63}Cu(\gamma,np)$ obtained by us from the data in Ref. [1] on the assumption that the cross-sections for both isotopes were similar in form has a value of 39 mb at its maximum at an energy of 21 MeV, whereas the cross-section for the same reaction taken from Ref. [2] has a value of only 14.5 mb at its maximum, which occurs at 23 MeV (the difference in the positions of the maxima seems to confirm the questionable nature of the similarity between the cross-sections for the different isotopes).

Secondly, in the region from threshold to 19 MeV (Fig. 1) the cross-section for $^{63}Cu(\gamma,np)$ from Ref. [2] has large negative (non-physical) values (up to -4.5 mb at 18 MeV, while at energies up to the threshold 12-16 MeV there is also a non-physical region of positive values up to 10 mb). The presence of these non-physical regions of cross-section values evidently indicates that the normalization used for the two cross-sections, as the difference between which the cross-section under discussion was obtained, is unreliable.

Thirdly, the cross-section for $^{nat}Cu(\gamma,np)$ reaction from Ref. [1] has a value of 57 mb at its maximum at 21 MeV whereas the cross-section for $^{nat}Cu((\gamma,n) + (\gamma,np))$ from Ref. [5] has a value of only 27 mb at this energy and the cross-section for $^{nat}Cu((\gamma,p) + (\gamma,np))$ from Ref. [6] a value of 32 mb.

A number of conclusions may be drawn from the foregoing:

- The cross-section for $^{nat}Cu(\gamma,np)$ from Ref. [1], has, on the whole, a regular shape (measurement of the yield curve, use of the photon difference method), but is greatly overestimated in value. Moreover, as a consequence of the large treatment step (2 MeV), the energy position of the cross-section has been determined only with an accuracy of up to 1 MeV;
- Evidently, the cross-section for the $^{nat}Cu(\gamma,np)$ cannot be used directly, taking into account only isotopic abundance, to obtain information on the cross-sections for the isotopes, owing to the differences in their energy positions;
- The presence of non-physical regions in the cross-section for the $^{63}Cu(\gamma,np)$ reaction points to the need for a new intercalibration and normalization of the cross-sections from Refs [2] and [5], and for recalculation of this cross-section.

COMBINED ANALYSIS AND EVALUATION

Cross-section for the $^{63}Cu(\gamma,np)$ reaction

It is evident that the cross-sections for the $^{63}Cu((\gamma,n) + (\gamma,np))$ and $^{63}Cu(\gamma,n)$ reactions in the region below the threshold of the (γ,np) reaction should coincide. However, it is clearly seen in Fig. 2 that there is a difference between the data from Refs [5] and [2] in this region as well. We therefore corrected the cross-section and energy scales for these

data in order to minimize the difference in their initial ranges. With this correction, the cross-sections from Refs [2] and [5] were assumed to be of the same value with regard to possible systematic uncertainties, and changes were therefore made to each of them. The procedure proposed in Ref. [6] was used for two steps of approximation. The new calibration was based on the energy weighting of the cross-sections in the region from 10.2 to 16.7 MeV (i.e. up to the threshold of $^{63}Cu(\gamma,np)$ reaction), while the integral cross-sections in the same region were used for the new normalization. The resulting change in these characteristics of the cross-sections is shown in Table 2, and the transformed cross-sections in comparison with each other are given in Fig. 3. During correction the value of the sum χ^2 for these cross-sections decreased by a factor of more than 3 (from 38.1 to 11.5 at 66 points in the region below the threshold).

TABLE 2. CHANGES IN THE PARAMETERS OF THE $^{63}Cu((\gamma,n) + (\gamma,np))$ [5] AND $^{63}Cu(\gamma,n)$ [2] REACTION CROSS-SECTIONS AFTER CALIBRATION AND NORMALIZATION

Ref.	Initial data		Calibration*		Normalization**	
	Integral cross-section MeV · mb	Energy weighting position, MeV	Integral cross-section, MeV · mb	Energy weighting position, MeV	Integral cross-section, MeV · mb	Energy weighting position, MeV
[5] [2]	195 (5) 175 (3)	14.76 (5) 14.93 (3)	175 (4) 198 (3)	14.85 (5) 14.85 (3)	186 (5) 186 (5)	14.85 (5) 14.85 (3)
Difference	20(6)	0.17	23 (5)	0.00(6)	0(6)	0.00(6)

Remarks:

* Cross-section energy shift, upwards by 0.3 MeV for Ref. [5] and downwards for Ref. [2].

** The data from Refs [5] and [2] multiplied by factors of 1.07 and 0.94, respectively.

The resulting cross-section for the $^{63}Cu(\gamma,np)$ reaction is given in Fig. 4, together with the same cross-section from Ref. [2]. It should be noted that after the correction was made the above-mentioned non-physical negative maximum in the initial part of the cross-section virtually disappeared (the integral cross-section in the part of negative values became 1.4 ± 1.3 mb instead of 5.9 ± 2.7 mb). It will also be seen that a value of about 5 mb was added to the main part of the cross-section, the addition being virtually uniform for all energies from the threshold to the maximum. This led to an increase in the integral cross-section by $\approx$ 30% and a shift in the energy weighting position by 0.5 MeV towards lower energies.

Table 3 gives the parameters of the $^{63}Cu(\gamma,np)$ reaction cross-section obtained by the above method and those of the $^{nat}Cu(\gamma,np)$ cross-section evaluated with its help.

TABLE 3. PARAMETERS OF EVALUATED CROSS-SECTIONS FOR THE $^{63,nat}Cu(\gamma,np)$ REACTIONS

Nucleus	Position of the maximum MeV	Cross-section at the maximum mb	Energy weighting position	Integral cross-section in the 16.5-24.5 MeV region MeV · mb
^{63}Cu	23.5	19.3 (23)	21.85 (15)	74.8 (42)
^{nat}Cu	23.0	13.0 (24)	21.68 (16)	54.1 (33)

Cross-section for the $^{65}Cu(\gamma,np)$ reaction

In the absence of data on the (γ,n) reaction for ^{65}Cu the cross-section for the (γ,np) reaction cannot be obtained by subtraction as in the case of ^{63}Cu. An attempt was therefore made to evaluate the $^{65}Cu(\gamma,n)$ cross-section with use of one of the curves describing the shape of smoothed resonance. The parameters of the curve were found from the initial part

of the cross-section for $((\gamma,n) + (\gamma,np))$, and the degree of its agreement with the cross-section was determined by the same operation as for ^{63}Cu, for which the cross-section of the (γ,n) reaction to be evaluated is known. The best value of the sum χ^2 from the Gaussian and Lorentzian curves was obtained for the Gaussian (122 compared to 154 at 149 points), and this curve was used subsequently for the evaluation.

After Gaussian approximation of the cross-section for $^{63}Cu((\gamma,n) + (\gamma,np))$ in the energy region below the threshold of the (γ,np) reaction and slightly above it - from 10 to 19 MeV - the Gaussian obtained bears a very close resemblance to the cross-section for $^{63}Cu(\gamma,n)$ right up to 22 MeV (Fig. 5). Figure 6 compares the two cross-sections for $^{63}Cu(\gamma,np)$, one obtained by the above method and the other obtained by subtracting the Gaussian from the $^{63}Cu((\gamma,n) + (\gamma,np))$ cross-section [5], the cross-sections (or differences) being given over the whole energy integral for the $^{63}Cu((\gamma,n) + (\gamma,np))$ cross-section, and not simply in the region above the threshold of the (γ,np) reaction. The difference between the cross-section and the Gaussian does not exceed 6 mb (the average absolute deviation in the region above the threshold is 3 mb), which is a good approximation for the cross-section value of 71 mb at the maximum. This enables the $^{65}Cu(\gamma,n)$ cross-section to be determined with a probable uncertainty of around 3 mb.

In order to evaluate the cross-section for the $^{65}Cu(\gamma,np)$ reaction, we took the $^{65}Cu((\gamma,n) + (\gamma,np))$ cross-section from Ref. [5]. The correction operation performed for the $^{63}Cu((\gamma,n) + (\gamma,np))$ cross-section (see Table 2) was repeated, since the data were obtained at the same facility and had similar systematic uncertainties.

In the Gaussian approximation of the $^{65}Cu((\gamma,n) + (\gamma,np))$ cross-section the initial range up to 13 MeV was not used because of the pronounced steps it contained, and the approximation was performed in the 13-19.5 MeV region, i.e. also up to an energy slightly

above the threshold of the (γ,np) reaction, as with the trial fit for the ^{63}Cu isotope. The result of the approximation, together with the ^{65}Cu((γ,n) + (γ,np)) cross-section smoothed with a 0.5 MeV step, is given in Fig. 7. It is clear from the figure that the ^{65}Cu(γ,np) cross-section lies more or less within the limits of the assumed accuracy ($\pm$ 3 mb), so that, we can only tentatively speak about two relatively weak maxima for this cross-section in the region of 18 and 22.5 MeV. Evidently, the obtained ^{65}Cu(γ,np) reaction cross-section can be assumed to have the shape of two wide maxima with amplitudes of around 6 and 8 mb at energies of 18 and 22.5 MeV, respectively, and regions of negative values with a maximum of up to 3 mb between them.

The evaluated data on the cross-sections of the (γ,np) reaction for the two isotopes ^{63,65}Cu were used to determine the parameters of the ^{nat}Cu(γ,np) reaction cross-section (Table 3).

CONCLUSION

By making a combined analysis of the data from various experiments and taking into account the systematic uncertainties in the absolute normalization and energy calibration of their results, we obtained new data on the energy dependences of the ^{63,65,nat}Cu(γ,np) reaction cross-sections in the giant dipole resonance region. The cross-sections contain almost no non-physical regions (positive values below the threshold and negative values above it) and are not inconsistent with the data on the cross-sections for other photonuclear reactions with copper nuclei.

REFERENCES

[1] BARBER, W.C., GEORGE, W.D., Phys. Rev. 116 (1959) 1551.

[2] SUND, R.E., BAKER, M.P., KULL, L.A., WALTON, R.B., Phys. Rev. 176 (1968) 1366.

[3] BERMAN, A.I., BROWN, K.L., Phys. Rev. 96 (1954) 83.

[4] KATZ, L., CAMERON, A.G.W., Can. J. Phys. 29 (1951) 518.

[5] FULTZ, S.C., BRAMBLETT, R.L., CALDWELL, J.T., HARVEY, R.R., Phys. Rev. 133 (1964) B1149.

[6] VARLAMOV, V.V., EFIMKIN, N.G., ISHKHANOV, B.S., SAPUNENKO, V.V., in Problems of Atomic Science and Technology, Ser. Nuclear Constants No. 1 (1993) 52 (in Russian).

[7] TANAKA, T., HIROOKA, M., TSUBOTA, H., SUGAWARA, M., Res. Rep. Lab. Nucl. Sci., Tohoku Univ. 14 (1981) 137.

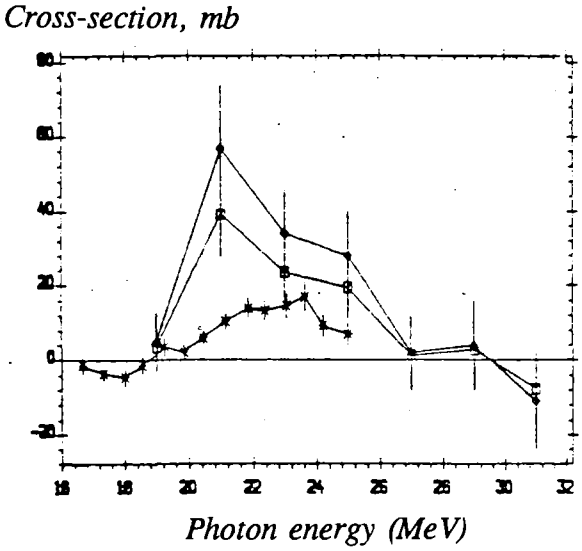

FIG. 1. *^{nat}Cu(γ,np) cross-section from Ref. [1] (diamonds), ^{63}Cu(γ,np) cross-section calculated from it by us (squares) and ^{63}Cu(γ,np) cross-section from Ref. [2] (stars).*

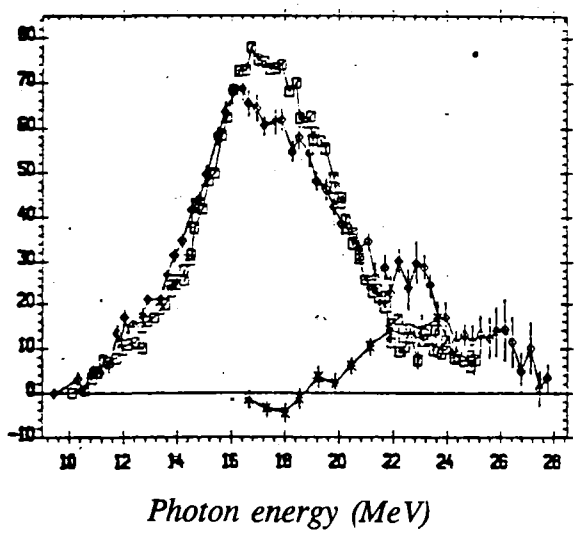

FIG. 2. *Comparison of the cross-sections for ^{63}Cu((γ,np) + (γ,np)) from Ref. [5] (diamonds), for ^{63}Cu(γ,n) from Ref. [2] (squares) and for ^{63}Cu(γ,np) from Ref. [2] (stars).*

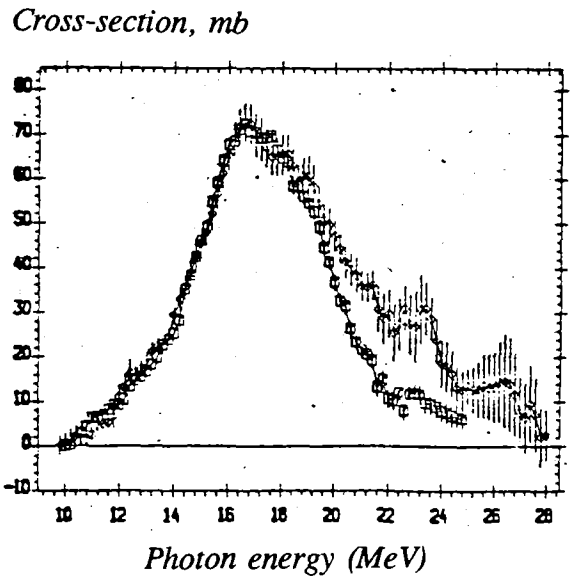

FIG. 3. Cross-section for ^{63}Cu((γ,n) + (γ,np)) [5] (diamonds) and ^{63}Cu(γ,n) [2] (squares) after re-normalization and re-calibration (initial data in Fig. 2).

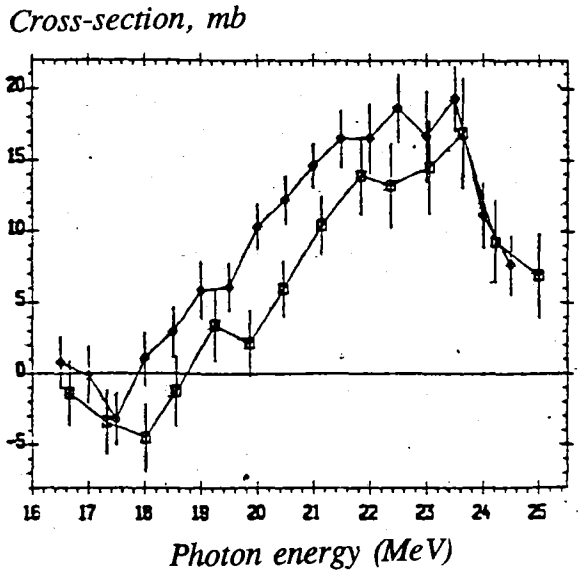

FIG. 4. The ^{63}Cu(γ,np) reaction cross-section obtained by us (diamonds) and data from Ref. [2] (squares).

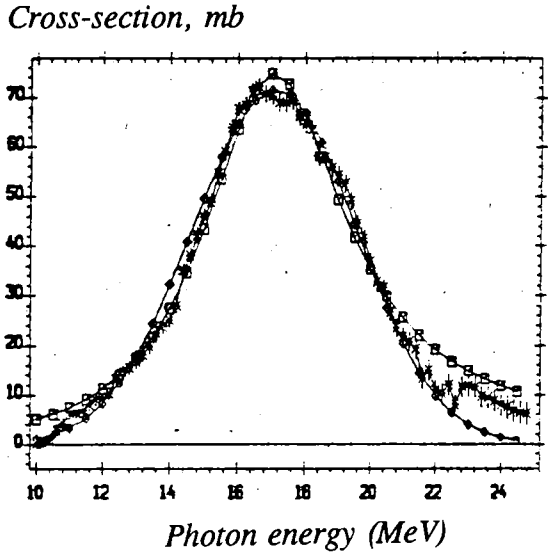

FIG. 5. Corrected $^{63}Cu(\gamma n)$ cross-sections (stars), with the Gaussian (diamonds) and Lorentzian (squares) curves obtained for the initial region of this cross-section (their parameters are, respectively: amplitudes 71.6 and 74.9 mb, ...[missing]

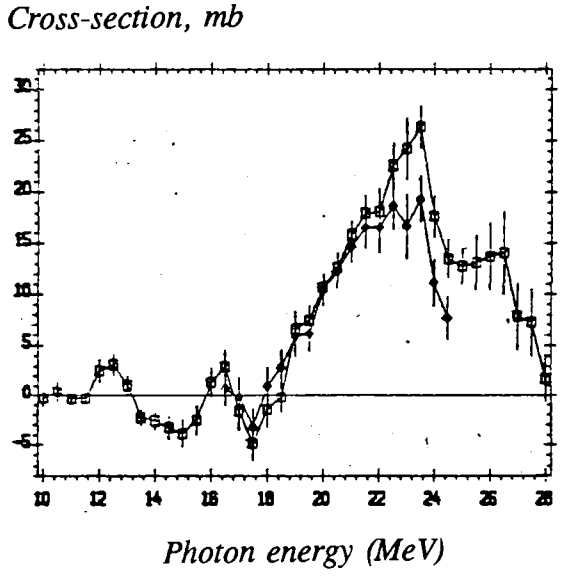

FIG. 6. Comparison of the evaluated $^{63}Cu(\gamma,np)$ cross-section (diamonds) and the cross-section obtained using the Gaussian curve (squares), in the whole energy interval of the initial cross-section for $^{63}Cu(\gamma,n)$.

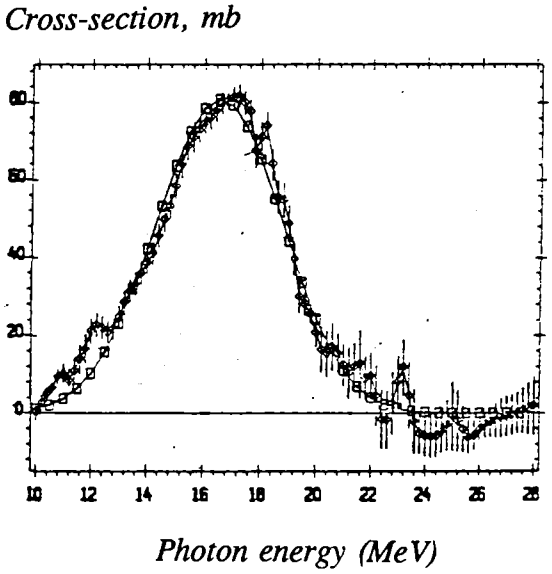

FIG. 7. Cross-section for the $^{65}Cu((\gamma,n) + (\gamma,np))$ reaction (diamonds) and Gaussian curve approximating it (squares), with the following parameters: amplitude 80.7 mb, position of maximum 16.6 MeV and width 2.2 MeV.

95-10765 (G)
Translated from Russian

UDC 539.171.401

INELASTIC SCATTERING OF NEUTRONS WITH EXCITATION OF THE MOST POPULATED LEVELS OF ^{138}Ba AND ^{141}Pr

L.A. Pobedonostsev and Ya.M. Kramarovskij
Khlopin Radium Institute
St. Petersburg

ABSTRACT

The method of associated gamma radiation has been used to determine the cross-sections for neutron inelastic scattering with excitation of the 1435 keV level for ^{138}Ba and the 1126 keV level for ^{141}Pr.

Nowadays, the neutron inelastic scattering cross-sections for most nuclei of structural components have been determined satisfactorily in the region of neutron energies located at the maximum of the fission spectrum. It does, however, seem likely that similar data will be required in future for nuclei located in the region of the fission product mass distribution maxima. This is due to the fact that improvement of nuclear reactors is to a considerable extent associated with the increase in the fuel burnup fraction which, in turn, results in an increase in the accumulation of fission products. Certain experimental difficulties arise, however, when studying inelastic scattering by such nuclei. These difficulties are mainly related to the sample, which can only be investigated in the form of a chemical compound, since most of these elements are chemically active. This, in turn, reduces the "substance under study" in the sample and complicates making corrections for finite geometry to the end result.

We have made an attempt to determine the inelastic scattering cross-sections with excitation of specific levels for ^{138}Ba and ^{141}Pr. The samples used were BaO and $Pr(NO_3)_3$,

which were poured in powder form into thin-walled Plexiglas containers with r = 16 mm and h = 33 mm. The total ^{138}Ba content in the sample was P = 24.84 g and the total ^{141}Pr content was P = 17.88 g. The samples were placed at a distance of 100 mm from the target. The level systems for ^{138}Ba and ^{141}Pr are sufficiently well known [1], but in the literature we could not find any data on neutron inelastic scattering cross-sections with excitation of specific levels for these nuclei.

As in our previous work [2, 3], we used the method of associated gamma-radiation to determine the (n,n′) reaction cross-sections. Neutrons were obtained in the T(p,n) reaction, and 0.3-0.5 mg/cm^2 thick titanium-tritium targets were used. An EhG-5 accelerator was used as a proton source with 20-25 μa beam currents. The neutron flux was determined using a miniature ionization chamber with a known quantity of ^{235}U on the basis of the fission fragment count; the ionization chamber was attached directly to the sample under investigation. Corrections for finite geometry were made to the end results. In these measurements the effect-to-background ratio is unfavourable in view of the small quantities of the substance under study. This makes it difficult to obtain a reliable determination of the (n,n′) reaction cross-sections with excitation of some specific levels. We therefore present the data on neutron inelastic scattering cross-sections with excitation of the most intensive levels.

REFERENCES

[1] DEMIDOV, A.M., GOVOR, L.I., CHEREPANTSEV, Yu.K., Atlas of Gamma-Radiation Spectra for Fast Neutron Inelastic Scattering in Reactors, Atomizdat, Moscow (1978) (in Russian).

[2] NEMILOV, Yu.A., KRAMAROVSKIJ, Ya.M., POBEDONOSTSEV, L.A., "Neutron Inelastic Scattering by ^{93}Nb", Problems of Atomic Science and Technology, No. 3 (1986) 24-26 (in Russian).

[3] POBEDONOSTSEV, L.A., NEMILOV, Yu.A., KRAMAROVSKIJ, Ya.M., "Neutron Inelastic Scattering by ^{52}Cr, ^{53}Cr and ^{27}Al Nuclei", Neutron Physics, Part 3 (1988) 226-231 (in Russian).

TABLE 1. CROSS-SECTIONS WITH EXCITATION OF LEVELS

^{138}Ba 1435 keV level		^{141}Pr 1127 keV level	
E, keV	σ_i, mb	E, keV	σ_i, mb
1720	239±20	1960	74±20
1760	347±25	2015	83±12
1810	565±40	2065	86±13
1870	570±40	2126	98±20
1920	616±45	2166	115±15
1960	634±45	2216	145±25
2010	570±45	2264	130±14
2070	483±40	2320	115±14
2120	460±40	2367	97±11
2170	441±35		
2220	411±35		

95-10765 (G)
Translated from Russian

UDC 539.172

EVALUATION OF THE (n,2n) REACTION CROSS-SECTION FOR ^{115}In AND ^{113}In

V.N. Manokhin
Institute of Physics and Power Engineering
Obninsk

ABSTRACT

An analysis has been made of the available evaluated and experimental data on the (n,2n) and (n,n′) reactions for ^{115}In and ^{113}In. The systematics have been used to evaluate the cross-sections for the (n,2n) reaction with formation of the isomeric levels for these isotopes.

The study of the excitation functions of the (n,2n) and (n,n′) reactions for isotopes of indium is of interest for the theory of nuclear reactions, and it can provide information on the dependence of the isomer ratios on the spin characteristics of levels. The ^{115}In(n,2n)^{114}In reaction is used in reactor dosimetry as a threshold detector for the unfolding of neutron spectra.

This paper attempts to analyse the available evaluated and experimental data on the (n,2n) and (n,n′) reactions for isotopes of indium, and to evaluate the ^{115}In(n,2n)^{114}In^{m} and ^{113}In(n,2n)^{112}In^{m} reactions.

Analysis of available data

The results of measurements and a comparative analysis of the (n,2n) and (n,n′) reaction cross-sections for ^{115}In and ^{113}In are given in Refs [1, 2]. One of the results of this analysis is the conclusion in Ref. [2] that there is a large difference between the (n,2n)

reaction cross-sections for the isotopes of indium (in the 14 MeV region, the (n,2n) cross-section for production of the isomeric state is 1100 mb for ^{113}In and 1300 mb for ^{115}In). The authors are of the opinion that this indicates a strong dependence of the cross-section on the spin of the isomeric level (4^+ for ^{113}In and 5^+ for ^{115}In).

However, on the basis of the systematics of the excitation functions and the systematics of the maximum cross-sections for the (n,2n) reaction proposed in Ref. [3], it can be demonstrated that this difference is not large.

To that end, an analysis was performed of both the (n,2n) and (n,n′) reaction cross-sections for the two isotopes in order to obtain a consistent description of all the values and thereby improve the reliability of the conclusions.

In Table 1 we give the cross-section values and isomer ratios from Refs [1, 2], which are compared with the evaluations of the (n,2n) reaction cross-sections at 14.1 MeV performed by us in the present work using the systematics from Ref. [3], with the (n,n′) reaction cross-sections for production of the ground state ($\sigma^{g}_{n,2n}$) and with the isomer ratios calculated on the basis of our evaluations of the (n,2n) reaction made in the present work.

The absorption cross-section values given in Table 1 were calculated by the formula from Ref. [2]. The $\sigma^{m}_{n,n'}$ cross-section was not evaluated but was taken from Refs [1, 2]. This cross-section accounts for less than 20% of the corresponding total cross-sections ($\sigma_m + \sigma_g$), and its uncertainty (no more than 10%) does not substantially affect the subsequent conclusions. The $\sigma^{g}_{n,n'}$ cross-section was obtained from the absorption cross-section by subtracting the cross-section of the (n,2n) reactions, the $\sigma^{m}_{n,n'}$ reaction cross-section and the cross-sections with charged-particle formation: since the (n,2n) reaction cross-section is dominant, $\sigma^{g}_{n,n'}$ depends strongly on its value. As we can see from Table 1, the difference in $\sigma^{m}_{n,2n}$ leads to a large difference in $\sigma^{g}_{n,n'}$ for both isotopes of indium.

The results of our evaluation of the (n,2n) reaction cross-sections give similar $\sigma^{g}_{n,n'}$ values and isomer ratios for both isotopes. These values seem more reasonable, since the ^{113}In and ^{115}In nuclei have identical spins of the ground and isomeric levels, and practically identical cross-sections of the (n,n') reaction with excitation of the isomeric levels of these nuclei. From this comparison we can conclude that the (n,2n) reaction cross-section for ^{113}In in Ref. [1] is too low, leading to an overestimation of $\sigma^{g}_{n,n'}$, and the (n,2n) cross-section for ^{115}In is too high, resulting in an underestimation of $\sigma^{g}_{n,n'}$ for this isotope.

Our evaluations of the (n,2n) reaction, which are given in Table 1 for an energy of 14.1 MeV, do not contradict the available experimental data; at the same time, with the help of these evaluations the cross-sections for the (n,2n) and (n,n') reactions with excitation of the ground and isomeric levels and the isomer ratios can be made consistent.

In Ref. [4], a description is given of the evaluation of the cross-sections for the (n,2n) reaction with excitation of the isomeric level of ^{115}In which was performed at the Nuclear Data Centre of the Atomic Energy Institute of the People's Republic of China for the IRDF-90 international dosimetric file. The analysis shows that, in this evaluation, the cross-section decreases above E_n = 15.3 MeV even though the competing (n,3n) reaction ($E_{th} \approx$ 16.5 MeV) begins to exert a noticeable influence on the behaviour of the (n,2n) cross-section at E_n > 17 MeV. Moreover, in the light of the above considerations concerning Ref. [2], the value of the cross-section in the 13-15 MeV region is a little too high.

TABLE 1. COMPARISON OF THE (n,2n) AND (n,n') REACTION CROSS-SECTIONS

Reaction	^{113}In (E_n = 14.1 MeV)		^{115}In (E_n = 14.1 MeV)		
	Cross-section, mb		Cross-section, mb		
	Ref. [1]	Present paper	Ref. [2]	Present paper	IRDF
Total absorption	1916	1916	1932	1932	
n,2n(m+g)	1340	1450	1570	1470	
n,2n(m)	1097	1190	1307	1220	1274[4]
n,2n(g)	245	260	263	250	
$\sigma_m/\sigma_m+\sigma_g$	0.82	0.82	0.83	0.83	
(n,n')/(m+g)	550	440	345	445	
n,n'(m)	57	57[1]	60	60[2]	
n,n'(g)	492	382	285	385	
$\sigma_m/\sigma_m+\sigma_g$	0.105	0.130	0.175	0.135	

Evaluation of the (n,2n) reaction cross-sections

We evaluated the excitation functions for the $^{115}In(n,2n)^{114}In^m$ and $^{113}In(n,2n)^{112}In^m$ reactions (see Figs 1 and 2 and Tables 2 and 3), using the systematics from Ref. [3]. The relative behaviour of the energy dependence of the cross-sections in the energy region from the reaction threshold to the energy where the cross-section maximum is observed was determined on the basis of the excitation function systematics, and the maximum cross-section of the reaction with isomeric state production at this energy was determined from the systematics of the maximum cross-sections using the experimental isomer ratio. This approach assumes that the isomer ratio remains constant over the whole energy range in question.

For ^{115}In, the total (n,2n) reaction cross-section, according to the systematics of the maximum (n,2n) reaction cross-sections [1], is 1570 mb in the 16-17 MeV region, where the threshold of the competing (n,3n) reaction lies. The maximum cross-section of the (n,2n) reaction with isomeric state production was calculated using the isomer ratio of 0.83 [1] and is 1300 mb. This value agrees satisfactorily with the available experimental data for this region. The parametrization of the energy dependence of the cross-section from the reaction threshold to the energy where the cross-section reaches a maximum (16-17 MeV) was carried out by normalizing the relative behaviour of the excitation function to the above value of 1300 mb, with some correction based on the available experimental data within the prediction uncertainty of the systematics. In the energy region above 17 MeV, competition from the (n,3n) reaction was taken into account, also on the basis of the systematics of the excitation function [3].

In the case of ^{113}In, the maximum (n,2n) reaction cross-section near the threshold of the (n,3n) reaction ($\approx$ 17 MeV) is 1550 mb according to the systematics. For an isomer ratio of 0.82 [2] the maximum cross-section of the ^{113}In(n,2n)^{112}In^{m} reaction is 1280 mb, and at 14.1 MeV it is 1190 mb. In the region above 17 MeV, competition from the (n,3n) reaction was taken into account. Figure 2 gives the curve from Ref. [5] in the 13-18 MeV neutron energy region for comparison. Clearly, in this instance too there is a tendency to underestimate the relative behaviour of the excitation function in the region above 15 MeV, even though the threshold of the competing (n,3n) reaction lies above 17 MeV. It should be noted that the data of P. Dekovskij shown in Fig. 2 were normalized by us to the isomer ratio of 0.82 [2].

The uncertainties of the evaluated data were determined as the uncertainties of the systematics of the excitation functions and are as follows:

Threshold-11.5 MeV	15%	15.0-17.0 MeV	3%
11.5-14.0 MeV	10%	17.0-18.0 MeV	5%
14.0-15.0 MeV	5%	18.0-20.0 MeV	10%

It is planned to include the evaluated cross-sections of the $^{115}In(n,2n)^{114}In^{m}$ reaction in the Russian dosimetric file (RDF-93).

TABLE 2. EVALUATED CROSS-SECTIONS FOR THE $^{115}In(n,2n)^{114}In^{m}$ REACTION

E_n, MeV	σ, mb	E_n, MeV	σ, mb
9.3	0	15.0	1280
9.5	30	15.5	1294
10.0	172	16.0	1300
10.5	365	16.5	1304
11.0	560	17.0	1300
11.5	726	17.5	1293
12.0	861	18.0	1270
12.5	981	18.5	1233
13.0	1080	19.0	1179
13.5	1162	19.5	1116
14.0	1220	20.0	1060
14.5	1258		

TABLE 3. EVALUATED CROSS-SECTIONS FOR THE $^{113}In(n,2n)^{112}In^{m}$ REACTION

E_n, MeV	σ, mb	E_n, MeV	σ, mb
9.7	0	15.0	1210
10.0	90	15.5	1238
10.5	214	16.0	1266
11.0	409	16.5	1276
11.5	533	17.0	1280
12.0	704	17.5	1280
12.5	805	18.0	1275
13.0	937	18.5	1262
13.5	1011	19.0	1233
14.0	1104	19.5	1182
14.5	1153	20.0	1132

REFERENCES

[1] CSIKAI, J., LANTOS Zs., BUCZKO, Cs.M., SUDAR, S., Neutron induced reaction cross-sections on ^{115}In at around 14 MeV, Report INDC(NDS)-232/L, Vienna (1990).

[2] BUCZKO, Cs.M., CSIKAI, J., CHIMOYE, T., JIMBA, B.W., "Cross-sections of ^{113}In(n,n')^{113}In^{m} and ^{113}In(n,2n)^{112}In^{m,g} reactions around 2 and 14 MeV neutron energies", Proc. Conf. on Nuclear Data for Science and Technology, Julich (1991).

[3] MANOKHIN, V.N., "Systematics of the excitation functions of the (n,2n) and (n,3n) reactions", Problems of Atomic Science and Technology, Series: Nuclear Constants 1 (1994) [in Russian].

[4] DUNJIU C., BAOSHENG, Y., ZISHENG, W., et al., Evaluation of the ^{115}In(n,2n)^{114}In^{m} Reaction Cross-Section, Report INDC(CPR)-024, Vienna (1991).

[5] WENRONG, Z., HANLIN, L., WEIXIANG, Yu., XIALIN, Yu., Compilation of Measurements and Evaluations of Nuclear Activation Cross-Sections for Nuclear Data Applications.

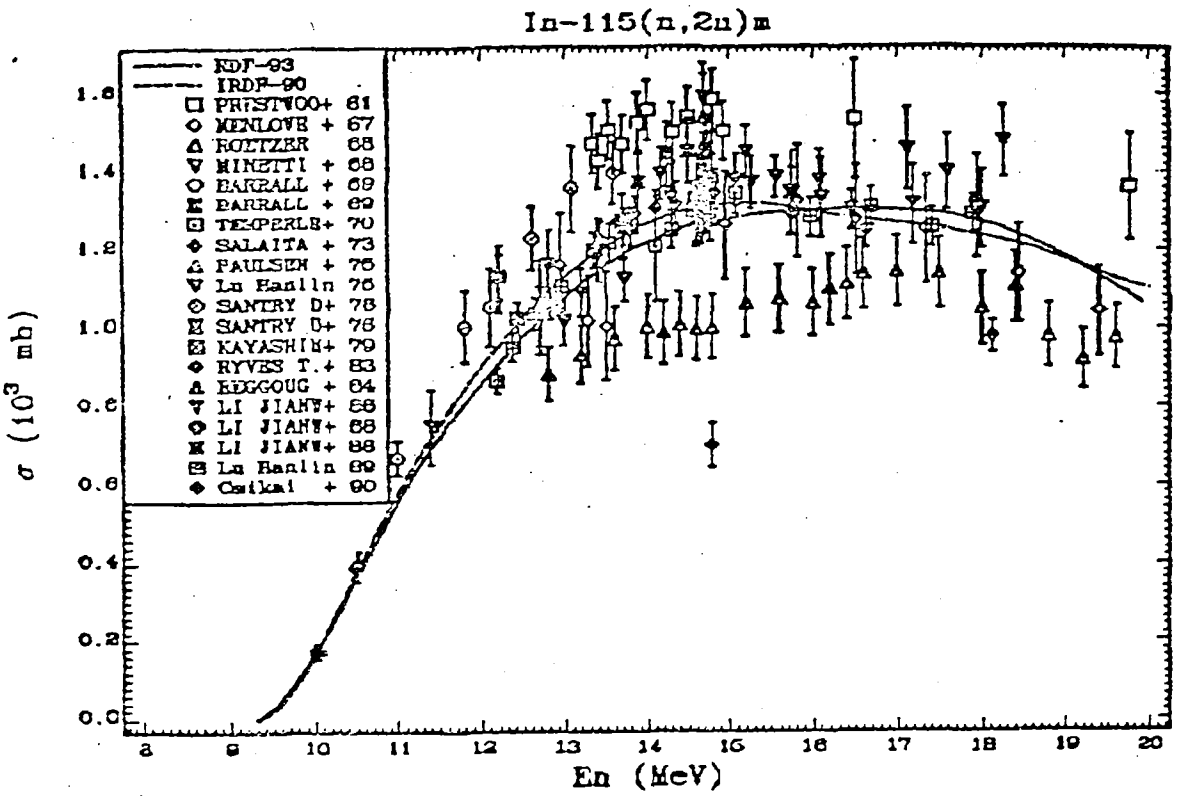

Fig. 1. Evaluation of the $^{115}In(n,2n)^{114}In^{m}$ reaction cross-section.

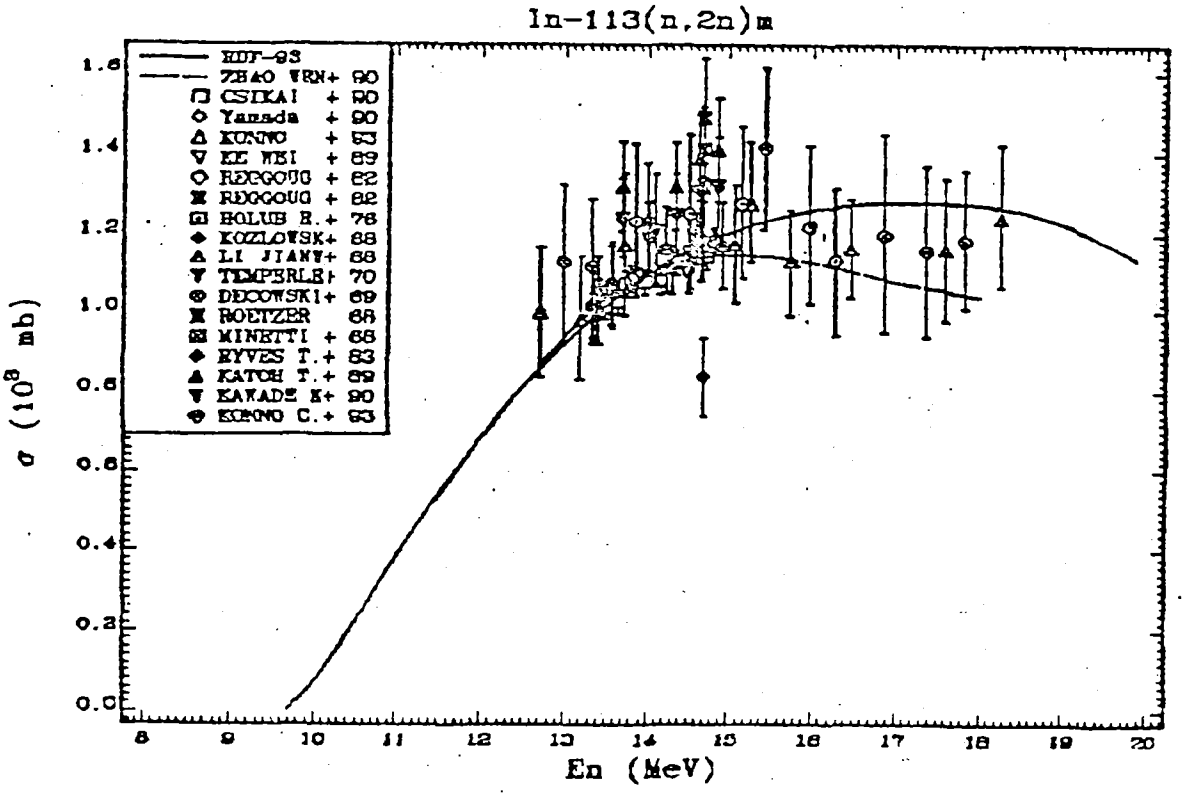

Fig. 2. Evaluation of the $^{113}In(n,2n)^{112}In^{m}$ reaction cross-section.

95-10765 (G)
Translated from Russian

UDC 539.172

INTEGRAL TESTING OF EVALUATED DATA FILES FOR SILICON, ZIRCONIUM AND NIOBIUM FROM THE BROND-2 LIBRARY

A.I. Blokhin and V.V. Sinitsa
Institute of Physics and Power Engineering, Obninsk

ABSTRACT

Data for Si, Zr and Nb materials from the BROND-2 library were tested through analysis of integral benchmark experiments with 14-MeV neutron sources. Intercomparisons of the calculated and experimental leakage neutron spectra from spherical assemblies are presented. Discrepancies between natural material and isotopes are demonstrated for the zirconium material. Important discrepancies for silicon data were revealed in the 14-MeV neutron source experiments.

INTRODUCTION

One of the stages of the International Thermonuclear Experimental Reactor (ITER) project is the creation of a comprehensive neutron data library for the basic components involved in the ITER design. Under the co-ordination of the IAEA's Nuclear Data Section, an international group of experts is setting up the FENDL-1 [1] evaluated neutron cross-section library, which includes neutron data files from the national libraries of the USA, Japan, Western Europe and Russia. The contribution from the Russian recommended neutron data library BROND-2 [2] to FENDL-1 is the data for deuterium, the ^{14}N and ^{15}N, silicon, ^{90}Zr, ^{91}Zr, ^{92}Zr, ^{94}Zr and ^{96}Zr, niobium and tin. The basic criteria for inclusion of data in the FENDL-1 library are given in Ref. [3]. One of the main stages in the assessment of evaluated nuclear data for the FENDL-1 library is testing the data by means of integral experiments carried out in simple geometry for the individual elements. At the last IAEA Advisory Group Meeting [4] a number of experiments, carried out at various facilities in different countries, were recommended as benchmark integral measurements. They include measurements made by the Japanese at the OKTAVIAN facility [5]. In the present paper we have made a comparative analysis of integral measurements [6] for the spectra of leakage neutrons from the surface of spherical samples and similar data obtained by calculation using evaluated neutron data from the BROND-2 library, for silicon, zirconium and niobium,

which are included in the FENDL-1 library. The results obtained can be used to evaluate the quality of the latest evaluated neutron data for the elements included in the FENDL-1 library, and also to suggest ways of improving these results.

EXPERIMENTAL DATA USED

The method employed to measure the spectra of leakage neutrons from spherical samples is described in Ref. [6]. The 14 MeV neutron source was a tritium target placed at the centre of the sphere under investigation and bombarded with 250 keV deuterons. The leakage neutron spectra were measured with an organic scintillator by the time-of-flight technique at an angle of 55° to the direction of the incident deuterons at a distance of 11 m from the centre of the sphere. The numerical experimental data on the leakage neutron spectra and also on the D-T neutron source spectra were obtained from Ref. [6].

CALCULATION METHOD

Using the GRUCON program package [7], we processed the nuclear data for silicon, niobium, zirconium and their isotopes to obtain the 175 group-averaged (vitamin-j) cross-sections at an ambient temperature of 300 K. The group constants and their functionals were prepared using the D-T neutron spectrum. The leakage neutron spectra were calculated out with the help of the ANISN program [8] in P5/S16 approximation. For zirconium the evaluated neutron data for individual isotopes were also checked for consistency with similar data prepared for a natural mixture. Figures 1-22 give the following data for silicon, zirconium and its isotopes, and niobium:

- Unshielded (solid line) and shielded (dashed line) total neutron interaction cross-sections and their ratio;

- Unshielded (solid line) and shielded (dashed line) neutron elastic scattering cross-sections and their ratio;

- Unshielded (solid line) and shielded (dashed line) neutron absorption cross-sections (sum of reactions with MT = 102-107) and their ratios;

- Neutron inelastic interaction cross-section (sum of reactions with MT = 4, 16, 22, 28);

- Leakage neutron spectrum for a sphere with diameter D, cm. Comparison of calculations (solid line) using the GRUCON/ANISN program package in (G175/P5/S16) approximation with experimental data [6]. The D-T neutron source spectrum is indicated by a broken line.

DISCUSSION OF RESULTS

Silicon. Figures 1-5 show the results of calculations for the silicon evaluated neutron data file from the BROND-2 library (MAT = 1402). Figure 5 gives calculations of the leakage neutron spectra for a sphere with a diameter D = 60 cm compared with experimental data. We note the presence of large discrepancies in the leakage neutron spectrum in the 100 keV-1 MeV region (Fig. 5), where of the neutron shielding effects for the absorption cross-section are substantial (Fig. 4). One possible explanation for these discrepancies may be that the data resolved and unresolved resonance parameters included in the file result in overestimation of the neutron shielding effect for absorption cross-section. Therefore the region below 1.0 MeV requires further analysis and, possibly modification of resonance parameters, mainly in the neutron radiative capture channel.

Zirconium and its isotopes. In Figs 6-17 we give the results of calculations for evaluated neutron data files for zirconium and its isotopes $^{90, 91, 92, 94\ 96}$Zr from the BROND-2 library (MAT = 4000, 4090, 4091, 4092, 4094 and 4096, respectively). Figures 6-9 show group cross-section data for natural zirconium, and Figs 9-15 similar results obtained from data files for individual isotopes compared with the results obtained from data files for the natural element. Figure 16 shows the calculations of neutron leakage spectra for a sphere with diameter D = 60 cm compared with experimental data. The calculations were carried

out both on the basis of the evaluated neutron data file for the natural element (solid curve), and on the basis of data files for the individual isotopes (dashed line). Figure 17 provides a more detailed comparison of the calculated leakage neutron spectra obtained on the basis of the data file for natural zirconium and its isotopes. On the whole, we can conclude that the description of the integral experiments is fully satisfactory both on the basis of the data file for the natural element and the data obtained from its isotopes. There were differences of up to 30% in the leakage spectra for these two sets of group cross-sections in the narrow band in the region of 10.0 MeV, which is attributable to a lack of consistency in neutron absorption cross-section data. A small inconsistency was, however, discovered - up to 17% in the elastic interaction cross-sections and up to 12% in the total cross-section - in the 200 keV-2.0 MeV neutron energy region between data for the natural element and those for its isotopes. Discrepancies in similar data for the inelastic scattering cross-section do not exceed 8% in the region above 10.0 MeV. It is also interesting to compare the results of calculation of the shielded cross-sections for natural zirconium performed by two different methods: direct summation the energy-dependent cross-sections and convolution of the moments using the Pade-2 approximation parameters (Figs 11, 13 and 15). Deviations in the shielded cross-sections in the 1.0-100.0 keV region ($\approx$ 2% in the elastic scattering and total cross-sections, and $\approx$ 20% in the absorption cross-section) are not attributable to differences in the initial cross-sections, as can be demonstrated by comparing the corresponding unshielded cross-sections (Figs 10, 12 and 14), but to inapplicability of the assumption that the effect of resonance overlap can be taken into account statistically. On the whole, we can conclude that at present the status of evaluated neutron data for zirconium and its isotopes is fully satisfactory for the purpose of describing the integral experiments investigated.

Niobium. Figures 18-22 show the results of calculations for the evaluated neutron data file for niobium from the BROND-2 library (MAT = 4193). Figure 22 shows calculations of the leakage neutron spectra for a sphere with diameter D = 28 cm compared with experimental data. The results presented for niobium on the whole are in satisfactory agreement with experiment. The sharp increase in the experimental data in the 100 keV region - the lower boundary of the measurement range - is probably due to inaccuracies in the experimental method and to the neutron detector's capabilities in this region. In any

case, the region below 150 keV requires additional experimental study. On the whole, we can conclude that at present the status of evaluated neutron data for niobium is entirely satisfactory for the purpose of describing the integral experiments in question.

CONCLUSION

The test results presented here for the evaluated neutron data files for silicon, niobium and zirconium on the basis of analysis of integral experiments on the spectra of leakage neutrons from the surface of spherical samples show that, on the whole, the status of data for zirconium and niobium is satisfactory. The neutron data file for silicon needs additional correction in the region below 1.0 MeV. Thus, continuation of work to modify the evaluated neutron data file for silicon is both very timely and necessary and will improve the accuracy of the evaluated data in the Russian BROND-2 library.

REFERENCES

1. Muir D.W., Ganesan S., Paschenko A.B., "FENDL: A reference nuclear data library for fusion applications". Inter. Conf. on Nuclear Data for Sci. and Tech., May 13-17, 1991, Juelich, Germany.
2. Blokhin A.I., Ignatyuk A.V., Kuz'minov B.D. et al. Proc. of Inter. Conf. on Nuclear Data for Sci. and Tech., May 13-17, 1991, Julich, Germany, p.800.
3. FENDL-2 and associated benchmark calculations. Summary report of the Advisory Group Meeting organized by the IAEA, Vienna, 18-22 November, 1991. Report INDC(NDS)-260, Vienna, IAEA, 1992, prepared by A.B.Paschenko and D.W.Muir.
4. Review of Uncertainty Files and Improved Multigroup Cross-Section Files for FENDL. Summary report of the IAEA Advisory Group Meeting organized by the IAEA in cooperation with the JAERI, R.,INDC(NDS)-297 (1994), prepared by S.Ganesan.
5. Sumita K. et al. Proc. of 12-th SOFT, vol.1, p.687 (1982).
6. Ichihara C. et al. Proc. of the 2-nd Spec. Meeting on Nuclear Data for Fusion Reactors. R., JAERI-M 91-062 (1991), p.255.

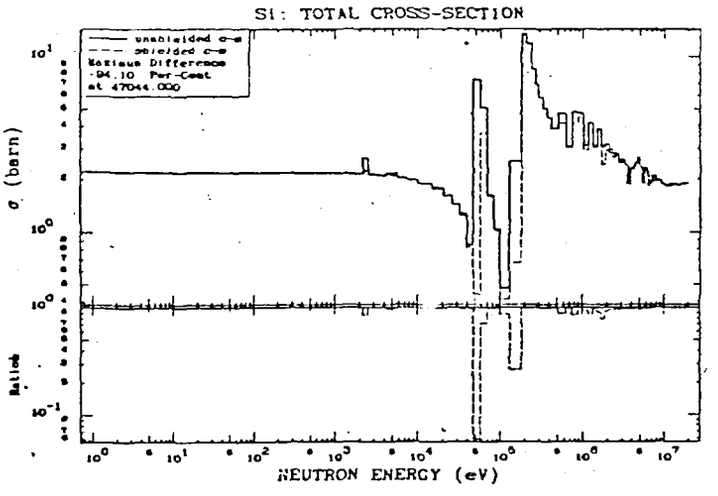

FIG. 1. *Silicon: unshielded (solid line) and shielded (dashed line) total neutron interaction cross-sections and their ratio.*

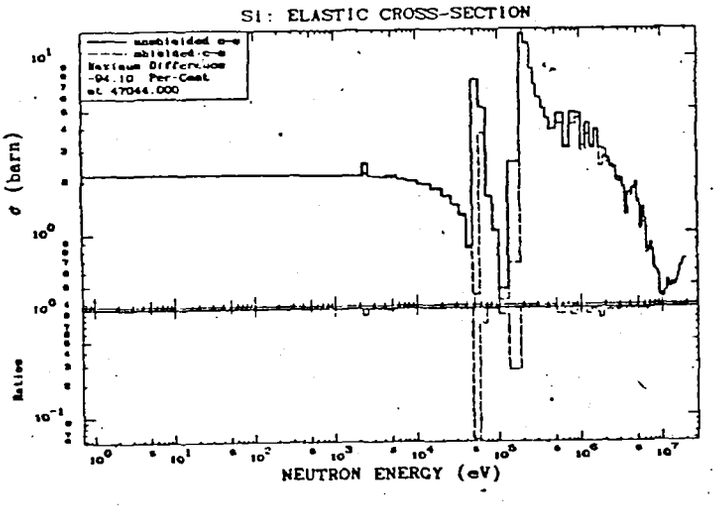

FIG. 2. *Silicon: unshielded (solid line) and shielded (dashed line) neutron elastic scattering cross-sections and their ratio.*

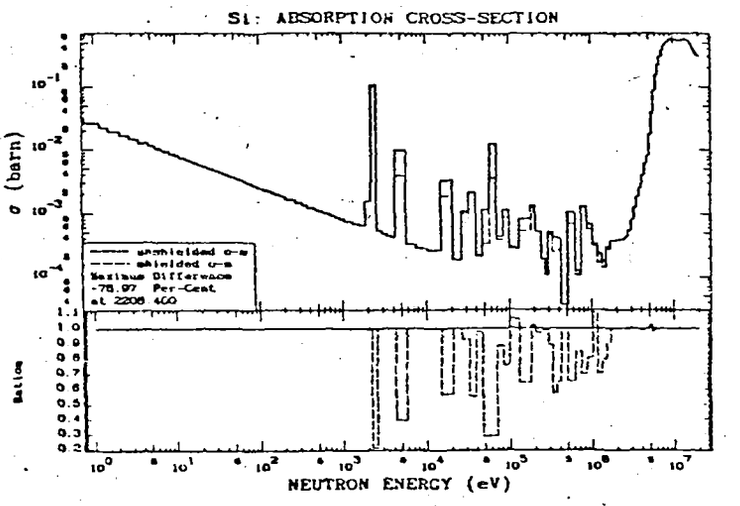

FIG. 3. *Silicon: unshielded (solid line) and shielded (dashed line) neutron absorption cross-sections (sum of reactions with MT = 102-107) and their ratio.*

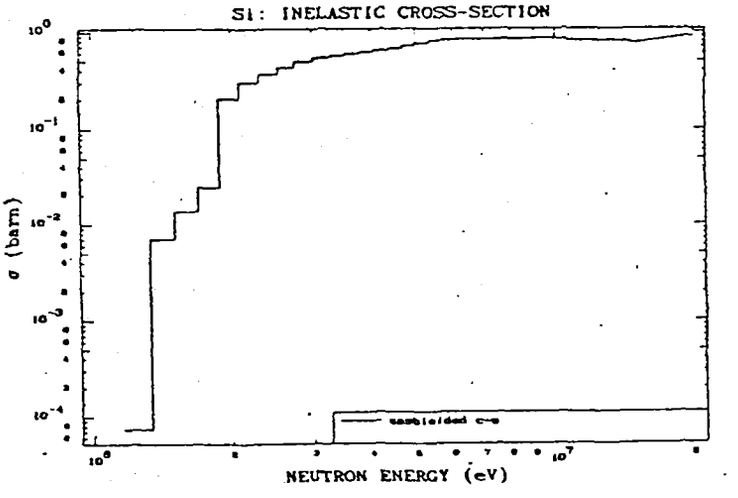

FIG. 4. *Silicon: neutron inelastic interaction cross-section (sum of reactions with MT = 4, 16, 22, 28).*

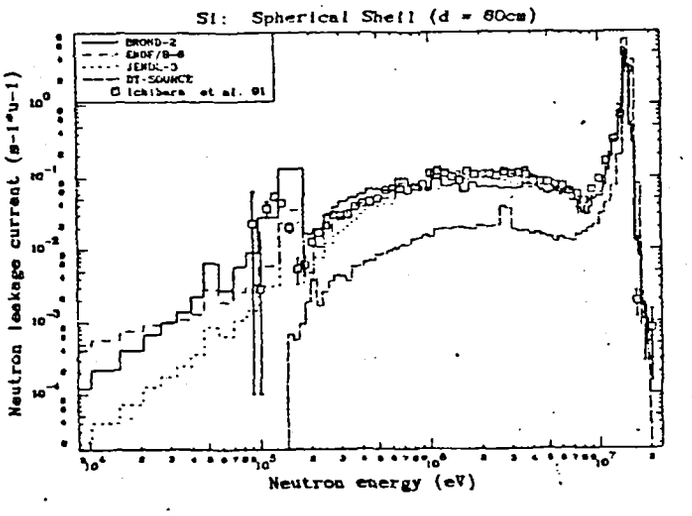

FIG. 5. *Silicon: leakage neutron spectrum for a sphere D = 60 cm. Comparison of GRUCON/ANISN (G175/P5/S16) calculations with experimental data [6]; the broken line shows the neutron source spectrum.*

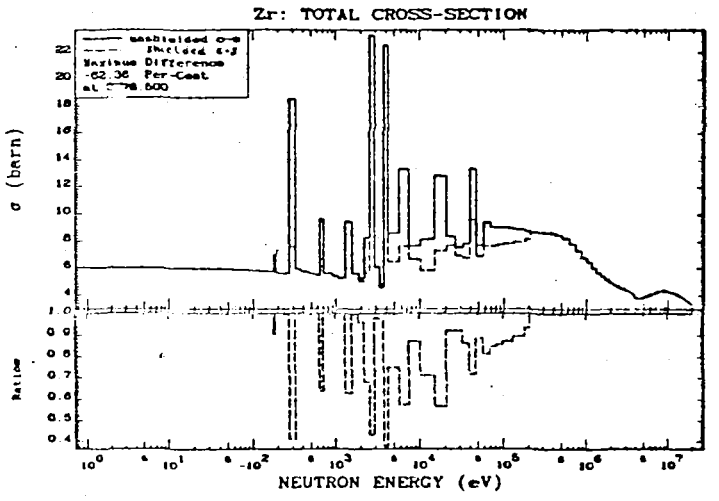

FIG. 6. *Zirconium: unshielded (solid line) and shielded (dashed line) total neutron interaction cross-sections and their ratio for natural material.*

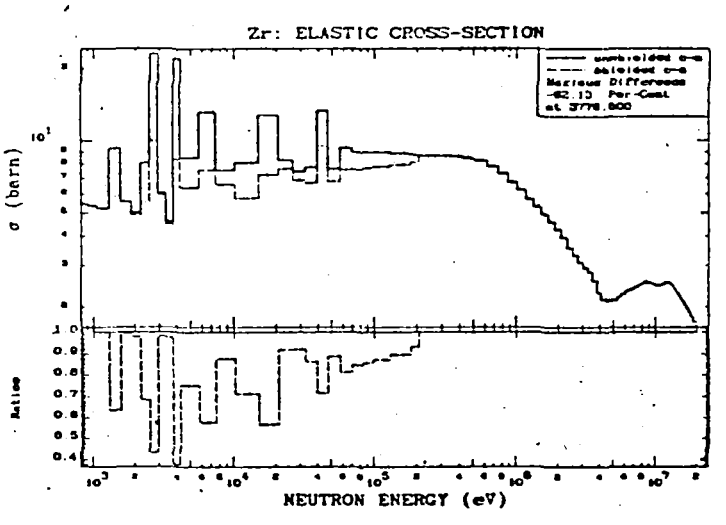

FIG. 7. *Zirconium: unshielded (solid line) and shielded (dashed line) neutron elastic scattering cross-sections and their ratio for natural material.*

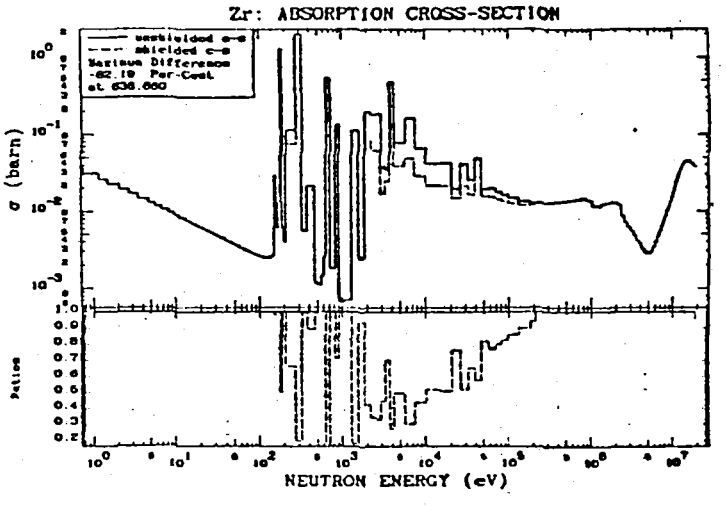

FIG. 8. *Zirconium: unshielded (solid line) and shielded (dashed line) neutron absorption cross-sections (sum of reactions with MT = 102-107) and their ratio for natural material.*

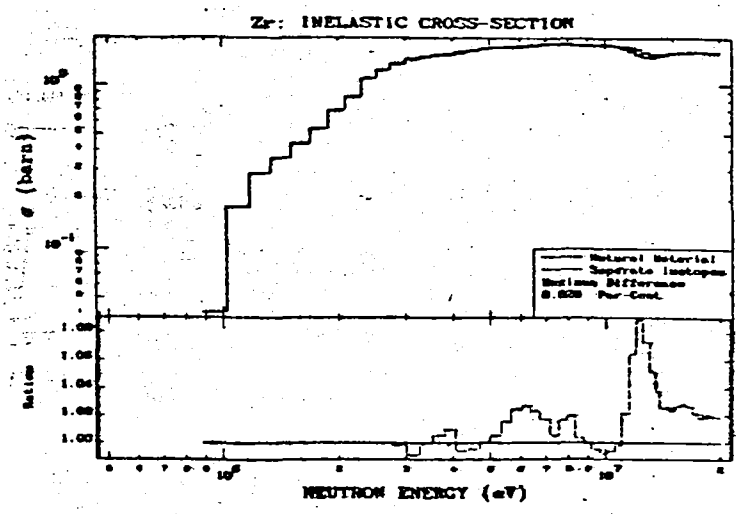

FIG. 9. *Zirconium: inelastic neutron interaction cross-section (sum of reactions with MT = 4, 16, 22, 28). Solid line: cross-section for natural zirconium; dashed line: cross-section obtained from data for isotopes; their ratio is shown in the lower part of the figure.*

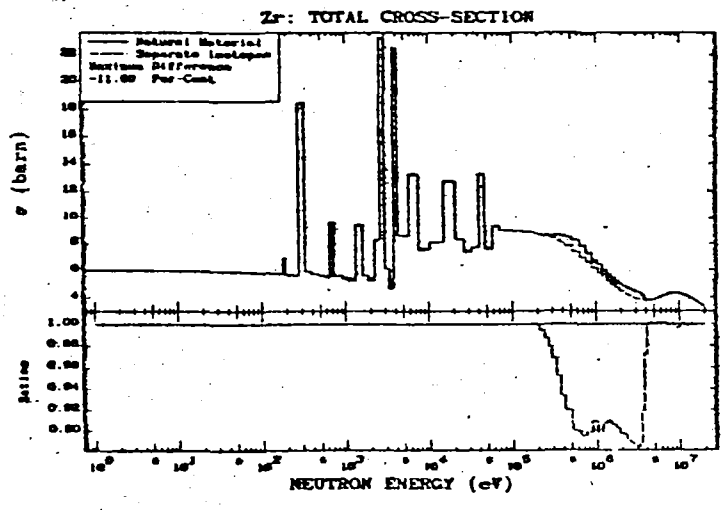

FIG. 10. *Zirconium: unshielded total neutron interaction cross-section, comparison of data for natural material (solid line) with data obtained for of isotopes (dashed line): their ratio is given in the lower part of the figure.*

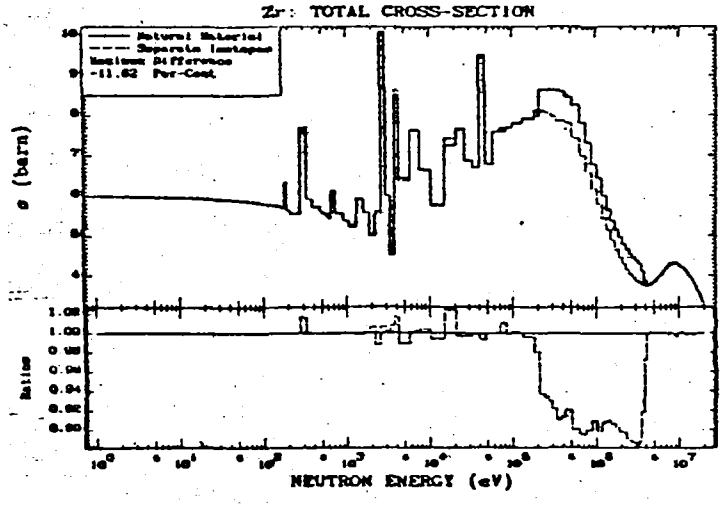

FIG. 11. *Zirconium: as in Fig. 10, but shielded total neutron interaction cross-section.*

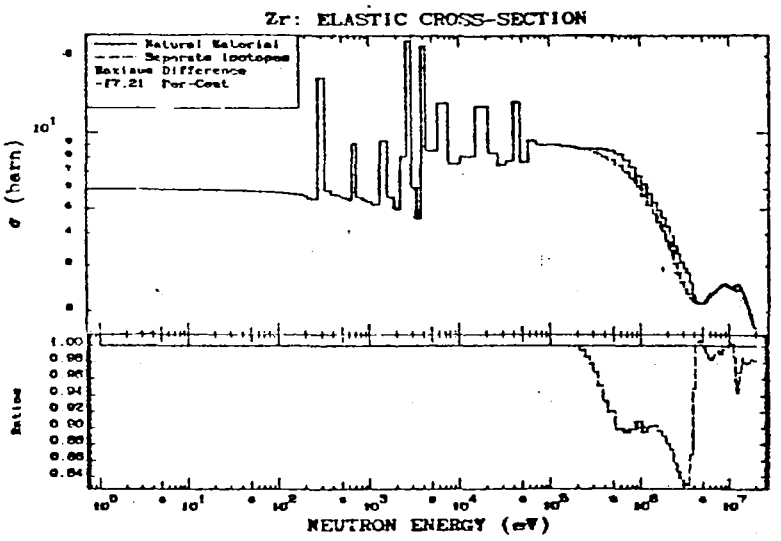

FIG. 12. *Zirconium: as in Fig. 10, but unshielded neutron elastic interaction cross-section.*

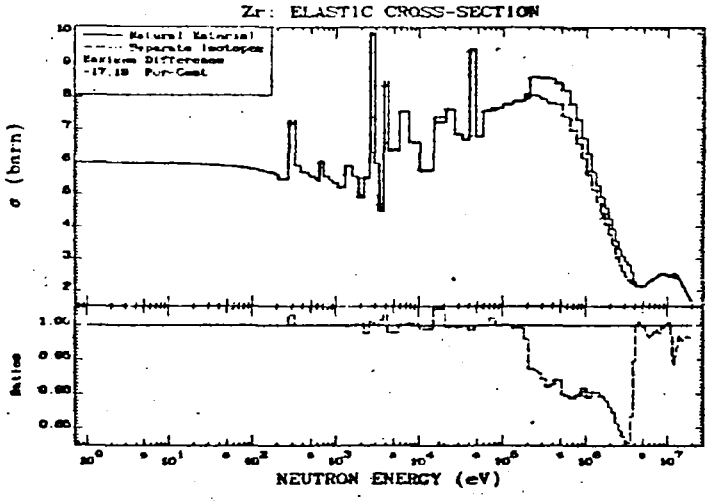

FIG. 13. *Zirconium: as in Fig. 10, but shielded neutron elastic interaction cross-section.*

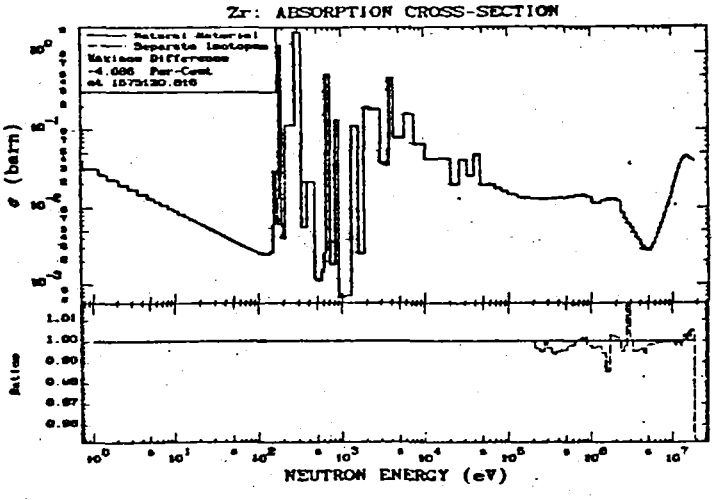

FIG. 14. *Zirconium: as in Fig. 10, but unshielded neutron absorption cross-section.*

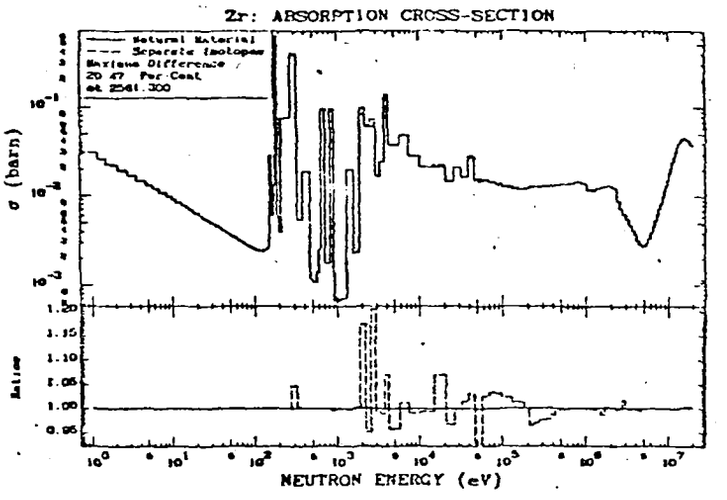

FIG. 15. *Zirconium: as in Fig. 10, but shielded neutron absorption cross-section.*

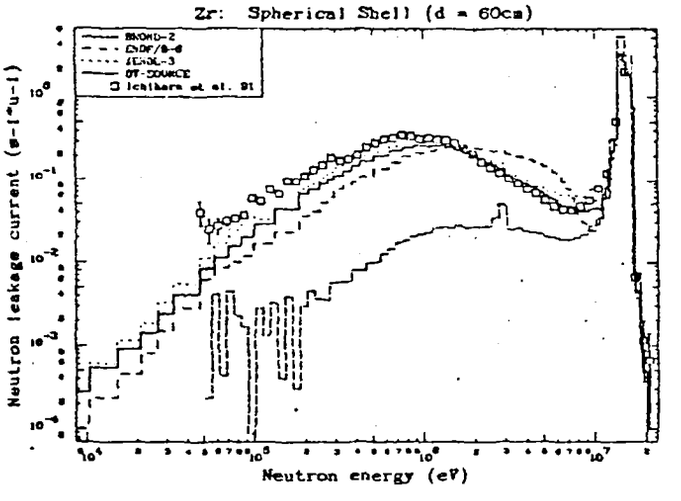

FIG. 16. *Zirconium: leakage neutron spectrum for a sphere with D = 60 cm. Comparison of GRUCON/ANISN (G175/P5/S16) calculations with experimental data [6]; solid line: calculation based on data for natural zirconium; dashed line: calculation based on data for isotopes separated out; dotted line: neutron source spectrum.*

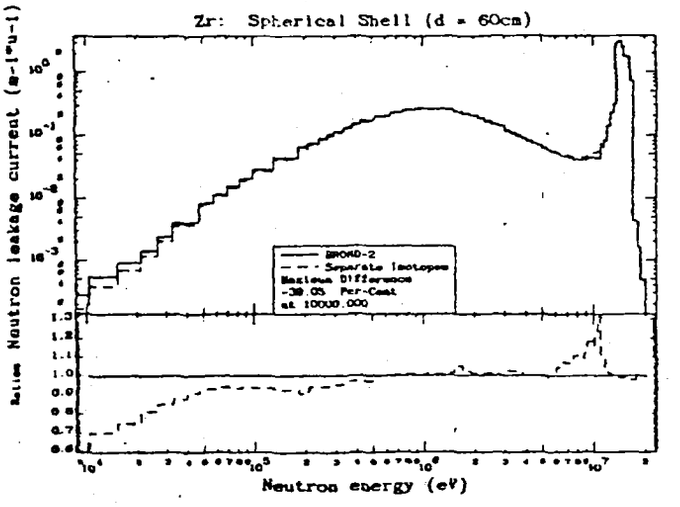

FIG. 17. *Zirconium: as in Fig. 16 but without comparison with experimental data. The lower part of the figure shows the ratio of calculated leakage neutron spectra obtained by two different methods.*

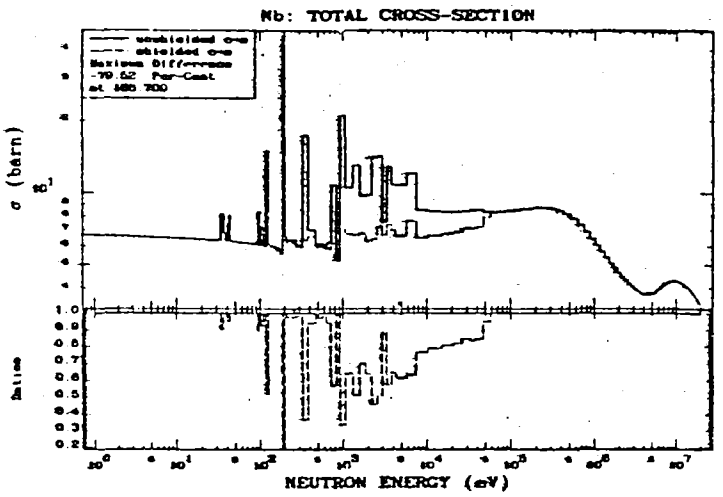

FIG. 18. *Niobium: unshielded (solid line) and shielded (dashed line) total neutron interaction cross-section and their ratio.*

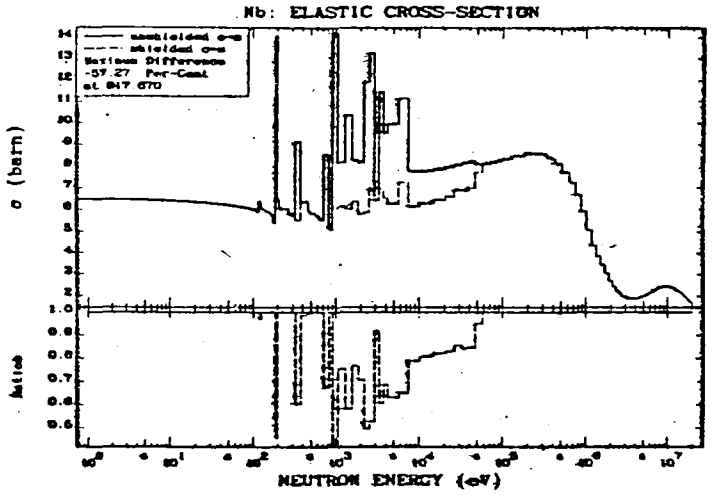

FIG. 19. *Niobium: unshielded (solid line) and shielded (dashed line) neutron elastic scattering cross-sections and their ratio.*

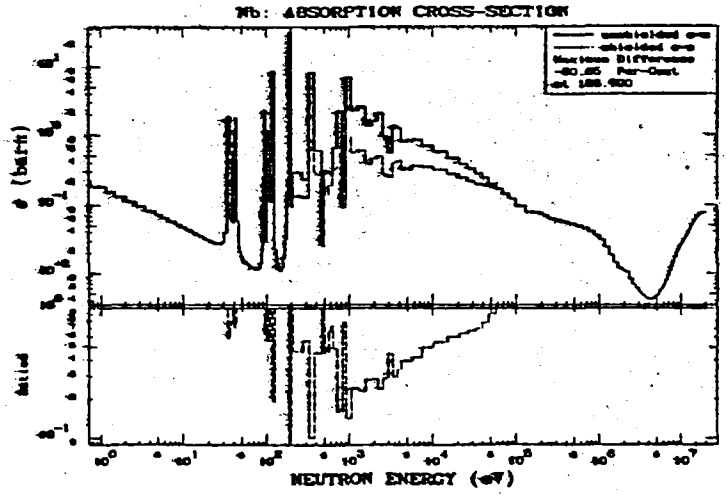

FIG. 20. *Niobium: unshielded (solid line) and shielded (dashed line) neutron absorption cross-sections (sum of reactions with MT = 102-107) and their ratio.*

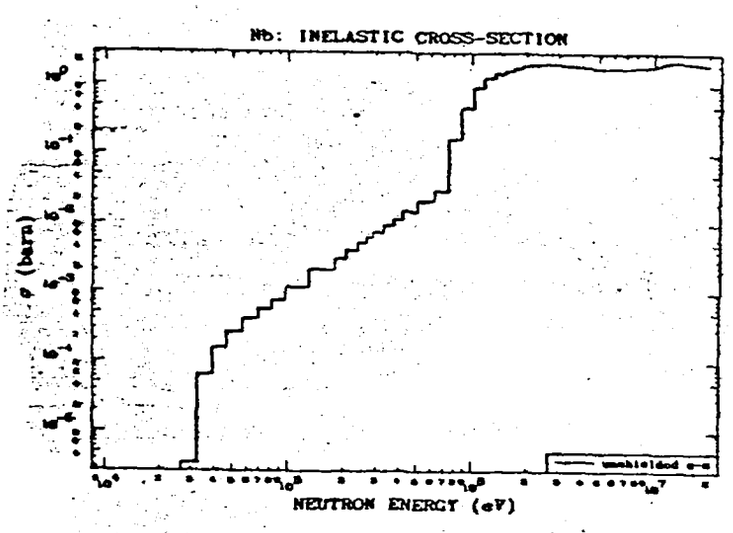

FIG. 21. *Niobium: neutron inelastic interaction cross-section (sum of reactions with MT = 4, 16, 17, 22, 28, 32, 33, 34).*

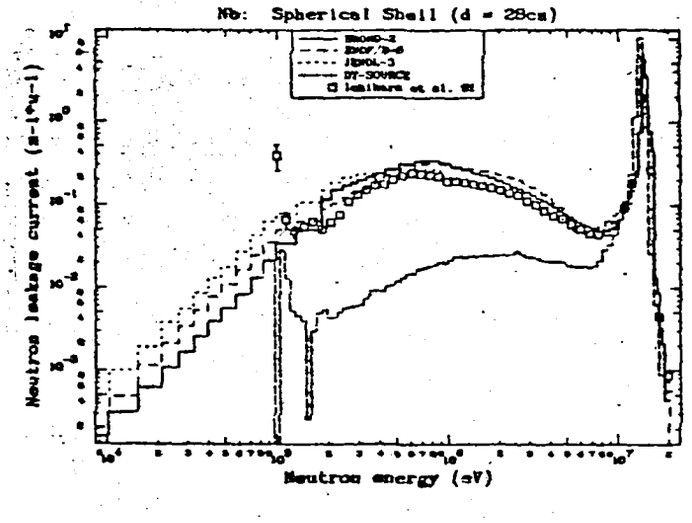

FIG. 22. *Niobium: leakage neutron spectrum for a sphere with D = 28 cm. Comparison of GRUCON/ANISN (G175/P5/S16) calculations with experimental data [6]; broken line shows the neutron source spectrum.*

95-10765 (H)
Translated from Russian

UDC 539.172

EVALUATION OF THE EXCITATION FUNCTION OF THE $^{141}Pr(n,2n)^{140}Pr$ REACTION FROM THE THRESHOLD TO 20 MeV

K.I. Zolotarev, V.N. Manokhin
Institute of Physics and Power Engineering
Obninsk

and

A.B. Pashchenko
International Atomic Energy Agency
Vienna

ABSTRACT

The paper gives the results of the evaluation of the $^{141}Pr(n,2n)^{140}Pr$ reaction cross-section in the neutron energy region from threshold to 20 MeV. This evaluation is based on experimental data and systematic behaviour of the (n,2n) reaction excitation functions. Using a generalized least square method the covariance matrix has been calculated. The evaluated cross-section data are presented in the ENDF/B-6 format.

The $^{141}Pr(n,2n)^{140}Pr$ reaction is sometimes used to monitor the 13-18 MeV neutron flux in measurements of the cross-sections for neutron reactions involving the formation of short-lived residual nuclei using the activation method [1, 2].

The $^{141}Pr(n,2n)^{140}Pr$ reaction is attractive to experimenters as a monitor for several reasons.

First of all, the cross-section for this reaction in the 13-18 MeV incident neutron energy region is considerably larger than for reactions such as $^{27}Al(n,p)^{27}Mg$ and $^{63}Cu(n,2n)^{62}Cu$, which are widely used to monitor neutron flux.

Secondly, in the neutron energy region in question, for the (n,2n) reaction cross-section for ^{141}Pr changes less than the cross-sections of the two reactions mentioned above, and this is a helpful characteristic for a monitor reaction. At E_n = 13 MeV, the cross-section for the $^{141}Pr(n,2n)^{140}Pr$ reaction is $\approx$ 1470 mb. As the neutron energy increases, the cross-section increases smoothly by only 20% to $\approx$ 1800 mb (E_n = 17.5 MeV) and then begins to drop gradually above 18 MeV as competition from the (n,3n) reaction increases. In the same energy interval (13-18 MeV), the cross-section for the $^{27}Al(n,p)^{27}Mg$ reaction changes by 50% (from 81 to 40.5 mb) and the cross-section for the $^{63}Cu(n,2n)^{62}Cu$ by 30% (from 275 to 781 mb).

Thirdly, ^{141}Pr is a monoisotope and ^{140}Pr can only be formed in the (n,2n) reaction channel.

Fourthly, from the point of view of the requirements for a monitor, the decay data for ^{140}Pr are known sufficiently well: $T_{1/2}$ = (3.39 $\pm$ 0.01) min, total intensity of positron emission $\sum_i \beta_i^+$ = 0.510 [3]. The 511 keV annihilation line dominates in the gamma radiation spectrum.

Fifthly, when ^{141}Pr is bombarded with 13-18 MeV neutrons, other reactions which lead to the formation of radioactive nuclei have very small cross-sections by comparison with the (n,2n) reaction. Therefore, for the first 10-15 minutes after the end of irradiation, the induced activity in the Pr samples will be determined mainly by the decay of the ^{140}Pr isotope formed in the (n,2n) reaction. This greatly simplifies the measurement procedure with a Pr monitor.

One of the main obstacles to using the $^{141}Pr(n,2n)^{140}Pr$ reaction as a monitor is the lack of sufficiently reliable data on the cross-section of this reaction.

The currently available evaluated data on the $^{141}Pr(n,2n)^{140}Pr$ reaction in the ENDF/B-6 [4], EAF-2 [5] and BOSPOR-86 [6] libraries show poor agreement with one another. Moreover, these libraries contain no information on uncertainties in the existing reaction cross-section data.

In this paper, we present the results of a new evaluation of the excitation function of the $^{141}Pr(n,2n)^{140}Pr$ reaction in the incident neutron energy range from the threshold to 20 MeV. The evaluation was performed on the basis of available microscopic experimental data on the reaction cross-section, together with additional information on the behaviour of the energy dependence of the cross-section obtained from the systematics of the (n,2n) reactions.

The evaluated curve of the excitation function of the $^{141}Pr(n,2n)^{140}Pr$ reaction and the covariance matrix of the uncertainty of the cross-sections were obtained using the database described below and the PADE-2 program [7].

Experimental data on the $^{141}Pr(n,2n)^{140}Pr$ reaction cross-section

Almost all the currently available microscopic experimental data on the $^{141}Pr(n,2n)^{140}Pr$ reaction cross-section were obtained before 1977 and the most intensive studies were carried out between 1960 and 1969. The experimental studies provide information on the excitation function of the (n,2n) reaction for ^{141}Pr in the 12.2-19.42 MeV incident neutron energy interval. In Table 1 we have listed all the studies known to us on measurement of the $^{141}Pr(n,2n)^{140}Pr$ reaction cross-section together with a short description of the experiments.

Table 1 does not mention the paper of R. Pepel'nik [24] published in 1989. This paper deals with the sensitivity of activation analysis using a high-flux source of 14 MeV

neutrons. It gives a value of 1660 mb for the $^{141}Pr(n,2n)^{140}Pr$ reaction cross-section without indicating the uncertainty, but it does not state how this value was obtained and what specific neutron energy it corresponds to. Therefore, we straightaway disregarded the data of this work.

From the experimental studies listed in Table 1 it is clear that most of the data was obtained in the 14-15 MeV interval and that there are no experimental data at all on the excitation function of the reaction in the energy region from the threshold up to 12.0 MeV. It will also be seen that all the measurements were performed by the activation method and that the $^{63}Cu(n,2n)^{62}Cu$ reaction was used most frequently as the reference reaction.

During the analysis, we corrected the original experimental data - where this was necessary and where the relevant information was available - in the light of new recommended data on the monitor (reference) reaction cross-sections and new recommended decay data for residual nuclei. Information on the recommended data used to correct the cross-sections is given in Table 2.

The measurement data of Wille and Fink [10], Rayburn (1961) [11], Khurana and Hans [12], Menon and Cuypers [16], Cuzzocrea et al. [17], Peto et al. [2], Bari [20], Araminowicz and Dresler [21] and Valkonen [23] were renormalized to the new data on the monitor reaction cross-sections.

Since information on the monitor reactions was incomplete, we did not attempt to correct the measurement data of Ferguson and Thompson [9], Koehler and Alford [13] and Sigg and Kuroda [22].

Ferguson and Thompson used the $^{6}Li(n,t)^{4}He$ reaction as a monitor. They took their data on the monitor reaction cross-section from Ref. [29]. In Ref. [29], the excitation function of the $^{6}Li(n,t)^{4}He$ reaction is given only in the form of a graph. It is therefore

difficult to estimate how strongly the monitor reaction cross-section data used in Ref. [29] differ from the data of Hale and Young, which are now accepted as standard [37].

Koehler and Alford measured the $^{141}Pr(n,2n)^{140}Pr$ reaction cross-section in the 12.2-18.15 MeV incident neutron region in relation to the absolute cross-section of this reaction for E_n = 14.4 MeV (σ = 1591 mb). They give no details as to how the absolute value of the $^{141}Pr(n,2n)^{140}Pr$ reaction cross-section at 14.4 MeV was obtained.

Sigg and Kuroda measured the (n,2n), (n,p) and (n,α) reaction cross-sections for a large number of isotopes at the 14.8 MeV point. They used three reactions to monitor the neutron flux: $^{27}Al(n,p)^{27}Mg$, $^{27}Al(n,\alpha)^{24}Na$, and $^{28}Si(n,p)^{28}Al$. However, it is not clear from the description of the experiment what monitor reactions specifically were used to determine the $^{141}Pr(n,2n)^{140}Pr$ reaction cross-section.

We were only able to find numerical data on the Rayburn experiment (1963) [15] in the EXFOR library. However, neither the EXFOR library nor Ref. [15], cited by the author, contain any information on the method used to determine the neutron flux.

The data from three experiments were corrected by us in the light of the new decay data for residual nuclei. The cross-sections measured by Ferguson and Thompson [9], Rayburn (1961) [11] and Menon and Cuypers [16] were corrected on the basis of the new recommended value for the total positron yield during the decay of ^{140}Pr [3]. In addition, Rayburn's data (1961) were corrected to take into account the new recommended value of the total positron yield for ^{62}Cu [25].

During the treatment of his experimental data, Rayburn used the value of $T_{1/2}$ = 3.13 min [11] for ^{140}Pr. This value is 8.3% lower than the recommended value [3]. Since we did not specifically know the time of irradiation of the Pr samples and the other time parameters, we were not able to correct Rayburn's data properly to take into account

the new, more accurate value of the half-life of ^{140}Pr. We therefore evaluated the influence of the difference in the half-life values on the cross-section value and accordingly increased the uncertainty in the cross-section value measured by Rayburn. For the same reason, we increased the uncertainty in the data of Wille and Fink [10] and Menon and Cuypers [16].

Araminowicz and Dresler only give the statistical component of the uncertainty for their measured value of the ^{141}Pr(n,2n)^{140}Pr reaction cross-section at E_n = 14.6 MeV. We evaluated the total uncertainty for the determination of the cross-section in this experiment. Account was taken of the uncertainties in the new data on the monitor reaction cross-section and in the recommended decay data for residual nuclei, in the data on the number of nuclei in the monitor and the sample, in the geometric parameters and in the various corrections.

Analysis of the experimental data shows that, with the exception of the 14-15 MeV interval, measurements performed by different authors are in satisfactory agreement one with another. In the 14-15 MeV interval to which, as we pointed out above, the largest body of experimental data pertains, the spread in the cross-section values obtained is found to be the greatest.

It should be noted that, owing to the large uncertainties in the reaction cross-section data, the measurements of Paul and Clarke [8] and of Wille and Fink [10] are of little use for evaluating the excitation function of the ^{141}Pr(n,2n)^{140}Pr reaction. However, we did not exclude the data of any measurements in the 14-15 MeV interval from the evaluation.

When preparing the database for the evaluation of the excitation function of the ^{141}Pr(n,2n)^{140}Pr reaction, the only thing we discarded from the whole set of experimental data was the first point in Rayburn's measurements [15]. The cross-section value of σ = (695 $\pm$ 70) mb at 12.3 MeV measured by Rayburn is greatly at variance with all the remaining experimental data obtained in the 12-13 MeV interval.

As we noted above, there are no experimental data on the $^{141}Pr(n,2n)^{140}Pr$ reaction cross-section in the 9.5-12.0 MeV region. Therefore, to evaluate the excitation function of the reaction in this region we used data obtained from the systematics of the (n,2n) reactions. Owing to the small amount of experimental data above 18 MeV, we also used information on the cross-section obtained from the systematics of the (n,2n) reactions.

Integral experimental data on the (n,2n) reaction cross-section for ^{141}Pr are available only for one type of neutron spectrum. Kohen measured the spectrum-averaged value of the $^{141}Pr(n,2n)^{140}Pr$ reaction cross-section for the spectrum of neutrons from a Be(d,n) source, obtaining $\sigma = (39 \pm 4)$ mb [30]. However, owing to the lack of detailed information on the neutron spectrum, these data are unsuitable for evaluating the excitation function of the $^{141}Pr(n,2n)^{140}Pr$ reaction.

Use of the systematics of the (n,2n) reactions to evaluate the shape of the excitation function

In Ref. [31], it is shown on the basis of the experimental data that the excitation functions of the (n,2n) reaction over a wide range of mass numbers have a practically identical shape in the incident neutron energy region from the reaction threshold E_{th} to E_{max}, where the cross-section reaches it maximum. The upper limit of this region is determined by the threshold of the competing (n,3n) reaction which, for ^{141}Pr, lies at $\approx$ 17.5 MeV. In the present work we evaluated the relative behaviour of the excitation function of the $^{141}Pr(n,2n)^{140}Pr$ reaction in the above energy region, using the systematics of the shape of the excitation functions. The excitation function was normalized with respect to the maximum cross-section evaluated with the help of the Padé approximation of the available experimental

data in the 12-18 MeV region. The value of the maximum cross-section (at $E_n \approx$ 16-17 MeV) is (1801.3 $\pm$ 54.0) mb and agrees satisfactorily with that calculated from the systematics of the maximum cross-sections for the (n,2n) reaction suggested in Ref. [31] for conditions where the (n,2n) reaction dominates and (n,3n) is the main competing reaction. These systematics are described by the dependence $\sigma_{n,2n}^{max} = 65.4 \cdot A^{2/3}$ and for ^{141}Pr they give a value of 1780 mb for the maximum cross-section.

The uncertainty of the relative behaviour of the proposed excitation function was determined from the spread of the experimental excitation functions which were normalized with respect to the maximum cross-section and (E_{max} - E_{th}) and on which the systematics were based. As the neutron energy changes from E_{th} to E_{max}, the uncertainty of the systematics of the shape decreases monotonically from $\approx$ 15% in the $\approx$ 0.5 MeV region near the threshold to zero at E_{max}. The total uncertainty of the absolute dependence of the cross-section is determined as the sum of the uncertainties of the shape and the normalization.

In the 17.5-20 MeV region, the behaviour of the reaction cross-section was evaluated with allowance for competition from the (n,3n) reaction. The energy dependence of the cross-section of this reaction was determined from the systematics of the shape of the (n,3n) reaction proposed in Ref. [31] on the basis of experimental data.

Statistical analysis of the cross-sections from the database

The method of statistical analysis of correlated data used to evaluate the excitation function of the ^{141}Pr(n,2n)^{140}Pr reaction was described in detail in Refs [32, 33]. Therefore, we shall only describe the basic features of the method.

The statistical analysis of the available reaction cross-section data was carried out using the non-linear regression model [34]. The following rational function (Padé approximation) was used as the model function:

$$f(E)=C+\sum_{i=1}^{l_1}\frac{a_i}{E-r_i}+\sum_{k=1}^{l_1}\frac{\alpha_k(E-\epsilon_k)+\beta_k}{(E-\epsilon_k)^2+\gamma_k^2}, \tag{1}$$

where E is the neutron energy and C, a_i, r_i, α_k, β_k, ϵ_k, γ_k are the parameters to be determined. The total number of parameters of the Padé approximation is:

$L = 2l_1 + 4l_2 + 1$.

The parameters of the model function are determined from the condition of minimum of the functional

$$S(\hat{\vec{\beta}}) = (\vec{\sigma}-\vec{f})^T(DPD)^{-1}(\vec{\sigma}-\vec{f}). \tag{2}$$

In expression (2) for the functional to be minimized $\hat{\vec{\beta}}$ is the vector of the parameters being determined, $\vec{\sigma}$ the vector of the cross-sections from the database, D the diagonal matrix of the uncertainty of the cross-sections from the database, P the correlation matrix of the experimental (calculated) data used to evaluate the excitation functions, and T means that the matrix is transposed.

The technical side of the minimization process, which is based on the discrete optimization method and the Newton-Gauss algorithm, is described in detail in Ref. [7].

The algorithm used for minimization of functional (2) contained two approximations appreciably simplifying the calculation scheme:

1. Cross-section data obtained in different experiments (calculations) were assumed to be uncorrelated;
2. The average correlation coefficient was used to describe the correlations between cross-sections obtained in the same experiment (calculation).

The covariance matrix of the uncertainties of the evaluated parameters $W(\hat{\bar{\beta}})$ and the uncertainties of the evaluated function at point $\Delta f\ (E_{i_k}^k, \hat{\bar{\beta}})$ are determined from the relations:

$$W(\hat{\bar{\beta}}) = \frac{S}{n-L}(X^T V^{-1} X)^{-1},$$

$$\Delta f\ (E_{i_k}, \hat{\bar{\beta}}) = \sum_{m=1}^{L} \sum_{j=1}^{L} X_{i_k m}^k X_{i_k j}^k W_{mj}$$

where n is the total number of data on the reaction cross-section used in the analysis and X the (n x L) matrix of the coefficients of the sensitivity of the rational function to a change in parameters $\left(X_{i_k m} = \frac{\partial f(E_{i_k}, \hat{\bar{\beta}})}{\partial \beta_m} \right)$.

Input data for the PADE 2 program

In order to evaluate the excitation function of the $^{141}Pr(n,2n)^{140}Pr$ reaction in the incident neutron energy range from the threshold to 20 MeV, we generated a database which included information on the reaction cross-section at 72 energy points. The excitation function values from the threshold to 12 MeV were taken from a calculation based on the systematics of the energy dependence of the (n,2n) reaction cross-sections.

The experimental database used by us to evaluate the excitation function of the $^{141}Pr(n,2n)^{140}Pr$ reaction is given in Table 3. It contains the original data of the different authors on the cross-sections and uncertainties, and the corrected values used in the evaluation.

To determine the average correlation coefficients, we analysed the structure of the uncertainties for all the experimental data.

The value of the average correlation coefficient $\overline{p^k}$ for the k-experiment containing information on the n_k-values of the reaction excitation function was determined by the formula

$$\overline{p^k} = \frac{2}{(n_k-1)\,n_k} \sum_{i=1}^{n_k-1} \sum_{j=i+1}^{n_k} \frac{\sum_{m=1}^{l} P_{ij}^m e_i^m e_j^m}{e_i e_j}, \qquad (3)$$

where $e_i(e_j)$ is the total uncertainty (standard deviation) of the cross-section at the i-th (j-th) point corresponding to a standard deviation of 1σ, $e_i^m(e_j^m)$ the m-th component of the systematic uncertainty of the cross-section at the i-th (j-th) point, P_{ij}^m the coefficient of the correlation between the m-th components of the systematic uncertainties at the i-th and j-th points and l the number of components of the systematic uncertainty.

The calculated data obtained from the systematics of the energy dependence of the (n,2n) reaction cross-sections were regarded as a single data set. Formula (3) was used to calculate the average correlation coefficient for these data in the same way as for the experimental data.

The average correlation coefficients for the $^{141}Pr(n,2n)^{140}Pr$ reaction cross-section data used are given in Table 4.

Results of evaluation of the excitation function

The statistical analysis of the information from the database showed that rational function (1) with parameters $l_1 = 1$, $l_2 = 1$, $C = 2054.62$, $a_1 = 300.36$, $r_1 = 20.871$, $\alpha_1 = 503.11$, $\beta_1 = 7419.1$, $\epsilon_1 = 9.3585$, $\gamma_1 = 1.9168$ best describes, from the physical point of view, the excitation function of the $^{141}Pr(n,2n)^{140}Pr$ reaction over the whole range of incident neutron energy from the threshold to 20 MeV. The cross-sections calculated by formula (1) with the above parameters are given in millibarns (mb). The neutron energy E is given in megaelectronvolts (MeV). The value of functional (2) which corresponds to the selected rational function is S = 1.423.

The results of the evaluation of the excitation function of the $^{141}Pr(n,2n)^{140}Pr$ reaction are shown in Fig. 1. This figure also gives the experimental data and shows the lower and upper boundaries of the uncertainty range of the evaluated curve which correspond to the standard deviation of 1σ. From Fig. 1 we can see that the experimental data of Wille and Fink [10], Khurana and Hans [12], Cevolani and Petralia [14], Menon and Cuypers [16], Peto et al. [2], Bari [20], and Araminowicz and Dresler [21], as well as the measurement data of Chatterjee et al. [19] at 14.2 and 14.5 MeV, do not fall within the uncertainty range of the evaluated excitation function. It should also be noted that the evaluated energy dependence of the $^{141}Pr(n,2n)^{140}Pr$ reaction cross-section in the 9.5-12.0 MeV energy range is determined to a considerable degree by the data obtained from the systematics of the (n,2n) reactions.

Figure 2 gives the data from our evaluation and the evaluated excitation functions for the $^{141}Pr(n,2n)^{140}Pr$ reaction from the ENDF/B-VI, EAF-2 and BOSPOR-86 libraries for comparison. Clearly, in the 13-18 MeV interval our evaluated data and the evaluated data from the BOSPOR-86 library show satisfactory agreement with one another. Of all the evaluations compared, the excitation function of the $^{141}Pr(n,2n)^{140}Pr$ reaction from the ENDF/B-VI library exhibit the worst agreement with experimental data. It should also be pointed out that the ENDF/B-VI value of the cross-section at the maximum of the excitation function (E_n = 17.5 MeV, $\sigma_{n,2n}$= 1984.3 mb) is 11% higher than the value given by the systematics of the (n,2n) reactions [31]. Moreover, the data from the ENDF/B-VI, EAF-2 and BOSPOR-86 libraries differ markedly from our evaluation of the excitation function near the threshold (9.5-12 MeV). As is mentioned above, our evaluation was obtained using the systematics of the shape of the (n,2n) reactions.

Data on the uncertainty of the evaluated excitation function of the $^{141}Pr(n,2n)^{140}Pr$ reaction in the different energy groups are given in Table 5. Table 5 shows that the highest accuracy in the evaluation of the reaction excitation function is achieved in the 13-18 MeV energy interval. The uncertainty in the reaction cross-section data in this energy interval is 2.45-3.0%.

The correlation matrix of the evaluated group cross-sections is given in Table 6. The strong positive correlation between the cross-section values in the region of the threshold and above 17.5 MeV is due to the dominant role played by data obtained from one source - the systematics of the shape of the (n,2n) reactions - in the evaluation of the cross-section in these regions.

As is mentioned above, there are at present no sufficiently reliable integral experimental data on the cross-section of the $^{141}Pr(n,2n)^{140}Pr$ reaction. For that reason, we

did not perform any testing of the evaluated excitation function with integral experimental data.

The spectrum-averaged values of the $^{141}Pr(n,2n)^{140}Pr$ reaction cross-sections for the ^{235}U fission neutron and ^{252}Cf spontaneous fission neutron spectra, calculated on the basis of our evaluated data, are (1.051 $\pm$ 0.044) mb and (1.917 $\pm$ 0.081) mb, respectively. In the calculation of the spectrum-averaged cross-sections, the data on the ^{235}U fission neutron spectrum were taken from the ENDF/B-VI library [35]. Mannhart's evaluation was used for the ^{252}Cf spontaneous fission neuron spectrum [36].

Conclusion

Additional information in the form of data from theoretical calculations using various models, or in the form of the systmatics of the cross-sections, is needed in order to evaluate the reaction excitation function when the experimental data show poor agreement or are lacking in individual energy regions.

The evaluation of the excitation function of the (n,2n) reaction for ^{141}Pr proposed in this work was made by simultaneously analysing the experimental data and data obtained from the systematics of the shape of the (n,2n) reactions. The evaluated data on the $^{141}Pr(n,2n)^{140}Pr$ reaction cross-section in the 13-18 MeV incident neutron region seem to us to be sufficiently reliable to enable them to be used as a reference cross-section in the measurement of the cross-sections of neutron reactions with the formation of short-lived residual nuclei.

Since the excitation function was evaluated in the region from the threshold to 20 MeV, the data of this evaluation can also be used both in neutron dosimetry and in solving various problems of activation calculation.

The present evaluation was used to generate a ^{141}Pr data file in ENDF-6 format, which includes: a short description of the evaluation, microscopic data on the (n,2n) reaction cross-section from the threshold to 20 MeV and the covariance matrix of the uncertainty of the cross-sections. We recommend this data file for inclusion in the Russian Dosimetric File (RDF-94).

In our opinion, a greater accuracy of the excitation function of the ^{141}Pr(n,2n)^{140}Pr reaction can be achieved only as a result of new experimental studies. The cross-sections need to be measured, first of all, in the 9.5-12 MeV region, and also above 18 MeV. Experiments to determine the spectrum-averaged cross-sections for the ^{235}U fission neutron and ^{252}Cf spontaneous fission neutron spectra may also make a substantial contribution to improving the accuracy of the reaction excitation function in the 10-15 MeV region.

References

1. Arnold D.M., Rayburn L.A. //Dissert. Abstract. - 1965. - V.26 P.3425.
2. Peto G. e.a. //Acta Physica Hung. -1968. - V.24.- P.93
3. Browne E., Firestone R.B. //Table of Radioactive Isotopes. - John Wiley & Sons, New York, 1986.
4. Schenter R.E. e.a. ENDF/B-VI Library, MAT=5925, Eval. Feb.1980
5. Kopecky J., Nierop D. //Contents of EAF-2. A Supplement to the EAF-2 Data File. Report ECN-I--91-053. Petten, July 1991.
6. Pashchenko A.B. e.a. Fast Neutron Activation Cross Section File. Report IAEA-NDS-96 (Rev.0), IAEA, Vienna, Oct. 1989.
7. Badikov, S., et al., The PADE2 Rational Approximation Program, Preprint FEhI-1686, Obninsk (1985) [in Russian].
8. Paul E.B., Clarke R.L. //Canadian J.Phys.. - 1953. - V.31. - P.267.
9. Ferguson J.M., Thompson W.E. //Phys.Rev.. - 1960. - V.118. -P.228.
10. Wille R.G., Fink R.W. //Phys.Rev. -1960. - V.118. - P.242.
11. Rayburn L.A. //Physical Review. - 1961. - V.122. -P.168.
12. Khurana C.S., Hans H.S. //Nucl.Phys. - 1961. - V.28. - P.560.
13. Koehler D.R., Alford W.L. Report NP-11667, 1962.
14. Cevolani M., Petralia S. //Nucl.Sci.Eng. -1962. - V.26 . - P.1328.
15. Rayburn L.A. //Bull.American Phys.Soc. - 1963. - V.8. - P.60.
16. Menon M.P., Cuypers M.Y. //Phys.Rev. -1967. - V.156. - P.1340.
17. Cuzzocrea P. e.a. //Nuovo Cimento. Sec.B. - 1967. - V.52, No.2. - P..476.
18. Bormann M. e.a. //Nucl.Phys. Sec.A. - 1968. - V.115. - P.309
19. Chatterjee A. e.a. Conf.,69ROORKEE, v.2, p.117, Dec.1969.
20. Bari A. //Dissert.Abst.- 1972. - Sec.B. - V.32. - P.5091.
21. Araminowicz J., Dresler J. //Prog.Rep. INR-1464. - May,1973. - P.14.
22. Sigg R.A., Kuroda P.K. //Inorg.Nucl.Chem.. - 1975 . - V.37. - P.631.
23. Valkonen M. Report JU-RR-1/1976, Jyvaeskylae University, 1976.
24. Pepelnik R. //Nucl. Instrum. and Methods. - 1989. - V.B40. - P.1205.
25. Ryves T.B. e.a. //Proc. of a Specialist's Meeting on Neutron Activation Cross Sections for Fission and Fusion Energy Applications. - ANL,USA, 13-15 September 1989. - P.65-68
26. Vonach H. The Al27(n,a)Na24 cross section. In Nuclear Data Standards for Nuclear Measurements. Report NEANDC-311 "U", 1992.
26. Wagner M. e.a. //Physics Data No.13-5, 1990.
27. Fu C.Y. e.a. ENDF/B-VI Library, MAT=2631, Eval. Mar.1989.
28. X-ray and gamma-ray standards for detector calibration. Report IAEA-TECDOC-619, IAEA, Vienna, September 1991.
29. Kern B.D., Kreger W.E. //Phys.Rev. - 1958. - V.112. - P.926.
30. Kohen B.L. //Phys.Rev. - 1951. - V.81. - P.184.
31. Manokhin, V.N., "Systematics of the excitation functions of the (n,2n) and (n,3n) reactions", Problems of Atomic Science and Technology, Ser. Nuclear Constants No.1 (1994) [in Russian].
32. Badikov, S.A., Zolotarev, K.I., Pashchenko, A.B., Evaluation of the $^{93}Nb(n,n')^{93}Nb^{m}$ Reaction Cross-Section from the Threshold to 20 MeV, Preprint FEhI-2252, Obninsk (1992) [in Russian].
33. Badikov S., Zolotarev K. //Proc. of NEANSC Specialist's Meeting on Evaluation and Processings of Covariance Data, Oak Ridge, USA, 1992, OECD, Paris, 1993, p.105.
34. Demidenko, E.Z., Linear and Non-linear Regression, Finansy i Statistika, Moscow (1981) [in Russian].
35. Weston L.W. e.a. Evaluated Neutron Data for U-235, ENDF/B-VI Library, MAT=9228, MF=5, MT=18, eval.apr. 1989.
36. Mannhart W. Report IAEA-TECDOC-410, p.158, IAEA, Vienna, 1987.
37. Hale, G.M., Young, P.G., The $^{6}Li(n,t)^{4}He$ Cross-Section in Nuclear Data Standards for Nuclear Measurements, Report NEANDC-311 "U" (1992) 22.

TABLE 1. EXPERIMENTS ON Pr141(n,2n)Pr140 REACTION

Energy range [MeV]	The number of points	Measurement method	Neutron flux monitor	Reference		
14.50 - 14.50	1	Act., Beta+	Long boron counter	Paul+	53	[8]
12.41 - 17.98	6	Act., NaI spectr.,coinc., Annih.Gamma	Li6(n,t)He4	Ferguson+	60	[9]
14.80 - 14.80	1	Act., Prop. counter, Beta	Cu63(n,2n)Cu62	Wille+	60	[10]
14.40 - 14.40	1	Act.,NaI(Tl) spectr.coinc.,Ann.Gamma	Cu63(n,2n)Cu62	Rayburn	61	[11]
14.80 - 14.80	1	Act., Geiger-Muller counter, Beta	Fe56(n,p)Mn56	Khurana+	61	[12]
12.20 - 18.15	8	Act.	Pr141(n,2n)Pr140 norm. at 14.40 MeV	Koehler+	62	[13]
14.13 - 14.13	1	Act., NaI, Annih.Gamma	Assoc.particles from T(d,n)He4 reaction	Cevolani+	62	[14]
12.30 - 17.80	20	Act., Spectr.coinc., Annih.Gamma	No information	Rayburn	63	[15]
14.50 - 14.50	1	Act., NaI(Tl), Annih.Gamma	Cu63(n,2n)Cu62	Menon+	67	[16]
14.00 - 14.00	1	Act., Geiger-Muller counter, Beta-	Cu63(n,2n)Cu62 and Cu65(n,2n)Cu64	Cuzzocrea+	67	[17]
12.78 - 19.42	10	Act., NaI, Annih.Gamma	H1(n,n)H1	Bormann+	68	[18]
15.00 - 15.00	1	Act., Spectr.coinc., Annih.Gamma	Cu63(n,2n)Cu62	Peto+	68	[2]
14.20 - 14.80	3	Act., NaI Spectr.coinc., Beta+	Absolut measurements	Chatterjee+	69	[19]
14.80 - 14.80	1	Act., Ge(Li), Gamma	Al27(n,a)Na24	Bari	72	[20]
14.60 - 14.60	1	Act., NaI, Gamma	Cu63(n,2n)Cu62	Araminowicz+	73	[21]
14.80 - 14.80	1	Act., Ge(Li), Gamma	Al27(n,p)Mg27 + 2 monitor reactions	Sigg+	75	[22]
14.70 - 14.70	1	Act., Ge(Li), Gamma	Al27(n,p)Mg27	Valkonen	76	[23]

TABLE 2. THE DATA USED AS STANDARDS FOR CORRECTIONS OF EXPERIMENTAL CROSS SECTIONS OF Pr141(n,2n)Pr140 REACTION

Reaction	Cross sections used as standards	Half-life	Radiation Mode and Energy	Intensity,%
Al27(n,p)Mg27	Ryves 89 [25]	9.462 (11) min	Gamma 843.7 keV	71.8 (4) [25]
Al27(n,a)Na24	Vonach 92 [26]	0.62356 (17) day	Gamma 1368.6 keV	99.9936 (15) [28]
Fe56(n,p)Mn56	ENDF/B-VI [27]	2.5785 (6) h	Gamma 846.8 keV	98.9 (3) [25]
Cu63(n,2n)Cu62	Ryves 89 [25]	9.74 (2) min	Beta+ 2927.1 keV	97.82 (4) [25]
Cu65(n,2n)Cu64	Ryves 89 [25]	12.701 (2) h	Beta+ 652.0 keV	17.87 (14) [25]
			Beta- 578.0 keV	39.04 (33) [25]
Pr141(n,2n)Pr140		3.39 (1) min	Beta+ 3388.0 keV	51.0 [3]

TABLE 3. CROSS SECTION DATA FOR THE REACTION Pr141(n,2n)Pr140

Nr.	E-Neutr [MeV]	Err. Centr [MeV]	Width [MeV]	Sigma (Orig) [mb]	Error (Orig) [mb]	Corr. Appl.	Sigma (Corr) [mb]	Error (Corr) [mb]	Reference
1	9.500	0.010	0.100	0.900	0.360	0	0.900	0.360	Systematics 94
2	9.600	0.010	0.100	8.500	1.700	0	8.500	1.700	Systematics 94
3	9.700	0.010	0.100	23.000	4.600	0	23.000	4.600	Systematics 94
4	9.800	0.010	0.100	50.000	10.000	0	50.000	10.000	Systematics 94
5	10.000	0.010	0.100	130.000	26.000	0	130.000	26.000	Systematics 94
6	10.500	0.010	0.100	420.000	63.000	0	420.000	63.000	Systematics 94
7	11.000	0.010	0.100	730.000	109.500	0	730.000	109.500	Systematics 94
8	11.500	0.010	0.100	990.000	148.500	0	990.000	148.500	Systematics 94
9	12.000	0.010	0.100	1200.000	120.000	0	1200.000	120.000	Systematics 94
10	12.200	0.030	0.150	1235.000	100.000	0	1235.000	100.000	Koehler+ 62
11	12.410	0.020	0.120	1231.000	111.000	3	1303.400	117.300	Ferguson+ 60
12	12.500	0.030	0.150	1580.000	155.000	0	1580.000	155.000	Koehler+ 62
13	12.780	0.010	0.110	1496.000	144.000	0	1496.000	144.000	Bormann+ 68
14	13.000	0.040	0.400	1403.000	140.300	0	1403.000	140.300	Rayburn 63
15	13.300	0.040	0.400	1475.000	147.500	0	1475.000	147.500	Rayburn 63
16	13.440	0.010	0.130	1485.000	143.000	0	1485.000	143.000	Bormann+ 68
17	13.500	0.050	0.500	1702.000	170.200	0	1702.000	170.200	Rayburn 63
18	13.700	0.030	0.150	1690.000	150.000	0	1690.000	150.000	Koehler+ 62
19	13.770	0.040	0.200	1386.000	125.000	3	1467.500	132.100	Ferguson+ 60
20	13.800	0.050	0.500	1769.000	176.900	0	1769.000	176.900	Rayburn 63
21	14.000	0.060	0.600	1916.000	191.600	0	1916.000	191.600	Rayburn 63
22	14.000	0.040	0.200	2002.000	225.000	1	1904.900	211.400	Cuzzocrea+ 67
23	14.050	0.020	0.100	1765.000	165.000	0	1765.000	165.000	Koehler+ 62
24	14.110	0.020	0.150	1614.000	159.000	0	1614.000	159.000	Bormann+ 68
25	14.130	0.020	0.100	1240.000	74.000	0	1240.000	74.000	Cevolani+ 62
26	14.200	0.050	0.500	2004.000	150.000	0	2004.000	271.000	Chatterjee+ 69
27	14.300	0.040	0.200	1790.000	160.000	0	1790.000	160.000	Koehler+ 62
28	14.300	0.060	0.600	2021.000	202.100	0	2021.000	202.100	Rayburn 63
29	14.400	0.030	0.300	1801.000	135.075	1 3 6	1641.700	119.844	Rayburn 61
30	14.500	0.050	0.500	2060.000	721.000	0	2060.000	721.000	Paul+ 53
31	14.500	0.030	0.300	1082.000	130.000	1 3 6	1172.900	143.100	Menon+ 67
32	14.500	0.050	0.500	2100.000	155.000	0	2100.000	281.000	Chatterjee+ 69
33	14.600	0.060	0.600	1902.000	190.200	0	1902.000	190.200	Rayburn 63
34	14.600	0.050	0.500	1347.000	115.000	1 6	1334.700	122.000	Araminowicz+ 73
35	14.700	0.050	0.500	1590.000	160.000	1	1683.000	111.000	Valkonen 76
36	14.740	0.050	0.270	1591.000	143.000	3	1684.600	151.600	Ferguson+ 60
37	14.800	0.080	0.800	2100.000	300.000	1 6	2271.900	331.700	Wille+ 60
38	14.800	0.050	0.500	1378.000	206.700	1	1167.800	175.170	Khurana+ 61
39	14.800	0.050	0.500	1780.000	110.000	0	1780.000	167.000	Chatterjee+ 69
40	14.800	0.040	0.200	1152.000	121.000	1	1141.000	104.000	Bari 72

TABLE 3. CROSS SECTION DATA FOR THE REACTION Pr141(n,2n)Pr140 (Continued)

Nr.	E-Neutr [MeV]	Err. Centr [MeV]	Width [MeV]	Sigma (Orig) [mb]	Error (Orig) [mb]	Corr. Appl.	Sigma (Corr) [mb]	Error (Corr) [mb]	Reference
41	14.800	0.040	0.200	1570.000	130.000	0	1570.000	130.000	Sigg+ 75
42	14.870	0.020	0.170	1700.000	164.000	0	1700.000	164.000	Bormann+ 68
43	14.900	0.060	0.600	1941.000	194.100	0	1941.000	194.100	Rayburn 63
44	15.000	0.060	0.300	2050.000	180.000	1	2145.000	150.000	Peto+ 68
45	15.200	0.060	0.600	1895.000	189.500	0	1895.000	189.500	Rayburn 63
46	15.400	0.070	0.700	1786.000	178.600	0	1786.000	178.600	Rayburn 63
47	15.520	0.020	0.170	1787.000	172.000	0	1787.000	172.000	Bormann+ 68
48	15.700	0.060	0.600	1857.000	185.700	0	1857.000	185.700	Rayburn 63
49	15.780	0.060	0.320	1737.000	156.000	3	1839.200	165.500	Ferguson+ 60
50	15.900	0.070	0.700	1867.000	186.700	0	1867.000	186.700	Rayburn 63
51	15.950	0.050	0.250	1775.000	160.000	0	1775.000	160.000	Koehler+ 62
52	16.180	0.020	0.180	1801.000	174.000	0	1801.000	174.000	Bormann+ 68
53	16.200	0.060	0.600	1778.000	177.800	0	1778.000	177.800	Rayburn 63
54	16.400	0.070	0.700	1701.000	170.100	0	1701.000	170.100	Rayburn 63
55	16.650	0.060	0.300	1830.000	160.000	0	1830.000	160.000	Koehler+ 62
56	16.800	0.060	0.600	1855.000	185.500	0	1855.000	185.500	Rayburn 63
57	16.850	0.020	0.180	1872.000	180.000	0	1872.000	180.000	Bormann+ 68
58	16.960	0.070	0.340	1606.000	145.000	3	1700.500	153.000	Ferguson+ 60
59	17.000	0.060	0.600	1764.000	176.400	0	1764.000	176.400	Rayburn 63
60	17.300	0.060	0.600	1802.000	180.200	0	1802.000	180.200	Rayburn 63
61	17.500	0.050	0.500	1840.000	184.000	0	1840.000	184.000	Rayburn 63
62	17.780	0.020	0.170	1905.000	183.000	0	1905.000	183.000	Bormann+ 68
63	17.800	0.020	0.200	1807.000	180.700	0	1807.000	180.700	Rayburn 63
64	17.980	0.050	0.240	1667.000	150.000	3	1765.100	158.900	Ferguson+ 60
65	18.000	0.010	0.100	1770.000	88.500	0	1770.000	88.500	Systematics 94
66	18.150	0.060	0.300	1830.000	160.000	0	1830.000	160.000	Koehler+ 62
67	18.500	0.010	0.100	1750.000	131.250	0	1750.000	131.250	Systematics 94
68	18.560	0.020	0.150	1853.000	178.000	0	1853.000	178.000	Bormann+ 68
69	19.000	0.010	0.100	1720.000	129.000	0	1720.000	129.000	Systematics 94
70	19.420	0.010	0.120	1804.000	174.000	0	1804.000	174.000	Bormann+ 68
71	19.500	0.010	0.100	1665.000	166.500	0	1665.000	166.500	Systematics 94
72	20.000	0.010	0.100	1600.000	160.000	0	1600.000	160.000	Systematics 94

CORRECTION CODES:
0) No correction applied
1) Cross-section renormalized to the new recommended values of reference cross-section used in measurement.
3) Cross-section renormalized to the new recommended decay data (Half-life, emission probability etc.)
6) Special correction. See text for details.

TABLE 4. AVERAGE CORRELATION COEFFICIENTS FOR DATA USED IN EVALUATION OF Pr141(n,2n)Pr140 EXCITATION FUNCTION

	Data		P^k		Data		P^k
1.	Paul+	53	0.00	10.	Cuzzocrea+	67	0.00
2.	Ferguson+	60	0.56	11.	Bormann+	68	0.62
3.	Wille+	60	0.00	12.	Peto+	68	0.00
4.	Rayburn	61	0.00	13.	Chatterjee+	69	0.00
5.	Khurana+	61	0.00	14.	Bari	72	0.00
6.	Koehler+	62	0.51	15.	Araminowicz+	73	0.00
7.	Cevolani+	62	0.00	16.	Sigg+	75	0.00
8.	Rayburn	63	0.25	17.	Valkonen	76	0.00
9.	Menon+	67	0.00	18.	Systematics		0.50

TABLE 5. EVALUATED GROUP CROSS SECTIONS AND THEIR UNCERTAINTIES FOR THE REACTION Pr141(n,2n)Pr140

Group-energy [MeV]		Group number	Cross sections [mb]	Uncertainty [mb]	Uncertainty [%]
9.50	10.00	1	47.29	8.08	17.09
10.00	10.50	2	269.11	41.81	15.54
10.50	11.00	3	576.67	64.26	11.14
11.00	11.50	4	866.64	67.50	7.79
11.50	12.00	5	1101.41	62.47	5.67
12.00	12.50	6	1280.56	55.60	4.34
12.50	13.00	7	1414.96	49.22	3.48
13.00	13.50	8	1515.89	44.37	2.93
13.50	14.00	9	1592.32	41.61	2.61
14.00	14.50	10	1650.73	40.89	2.48
14.50	15.00	11	1695.69	41.63	2.45
15.00	15.50	12	1730.34	43.09	2.49
15.50	16.00	13	1756.84	44.68	2.54
16.00	16.50	14	1776.61	46.13	2.60
16.50	17.00	15	1790.48	47.58	2.66
17.00	17.50	16	1798.72	49.72	2.76
17.50	18.00	17	1800.97	54.04	3.00
18.00	19.00	18	1787.98	69.53	3.89
19.00	20.00	19	1707.25	106.88	6.26

TABLE 6. CORRELATION MATRIX OF THE EVALUATED GROUP CROSS SECTIONS FOR THE REACTION Pr141(n,2n)Pr140 (correlations are given in percents)

Group-energy [MeV]		Group number	1	2	3	4	5	6	7	8	9	10	11	12	13	14	15	16	17	18	19
9.50	10.00	1	100																		
10.00	10.50	2	96	100																	
10.50	11.00	3	90	97	100																
11.00	11.50	4	78	87	96	100															
11.50	12.00	5	62	72	86	96	100														
12.00	12.50	6	46	54	71	87	97	100													
12.50	13.00	7	32	39	56	74	89	97	100												
13.00	13.50	8	22	27	42	60	76	89	97	100											
13.50	14.00	9	16	19	30	46	62	76	88	97	100										
14.00	14.50	10	15	15	22	34	47	62	76	89	97	100									
14.50	15.00	11	17	15	18	25	35	48	63	78	91	98	100								
15.00	15.50	12	22	18	18	20	27	38	52	68	83	93	99	100							
15.50	16.00	13	27	23	20	19	23	31	44	60	76	88	96	99	100						
16.00	16.50	14	34	29	25	22	23	29	40	55	70	83	91	96	99	100					
16.50	17.00	15	41	37	32	28	27	30	39	51	65	77	86	92	96	99	100				
17.00	17.50	16	48	44	41	37	34	35	40	49	60	69	77	84	89	94	98	100			
17.50	18.00	17	53	51	49	47	44	42	44	48	53	59	65	71	77	83	91	97	100		
18.00	19.00	18	55	55	58	60	58	53	48	44	41	39	39	42	48	56	67	80	92	100	
19.00	20.00	19	55	56	61	64	62	56	48	38	29	22	18	17	20	26	36	49	64	83	100

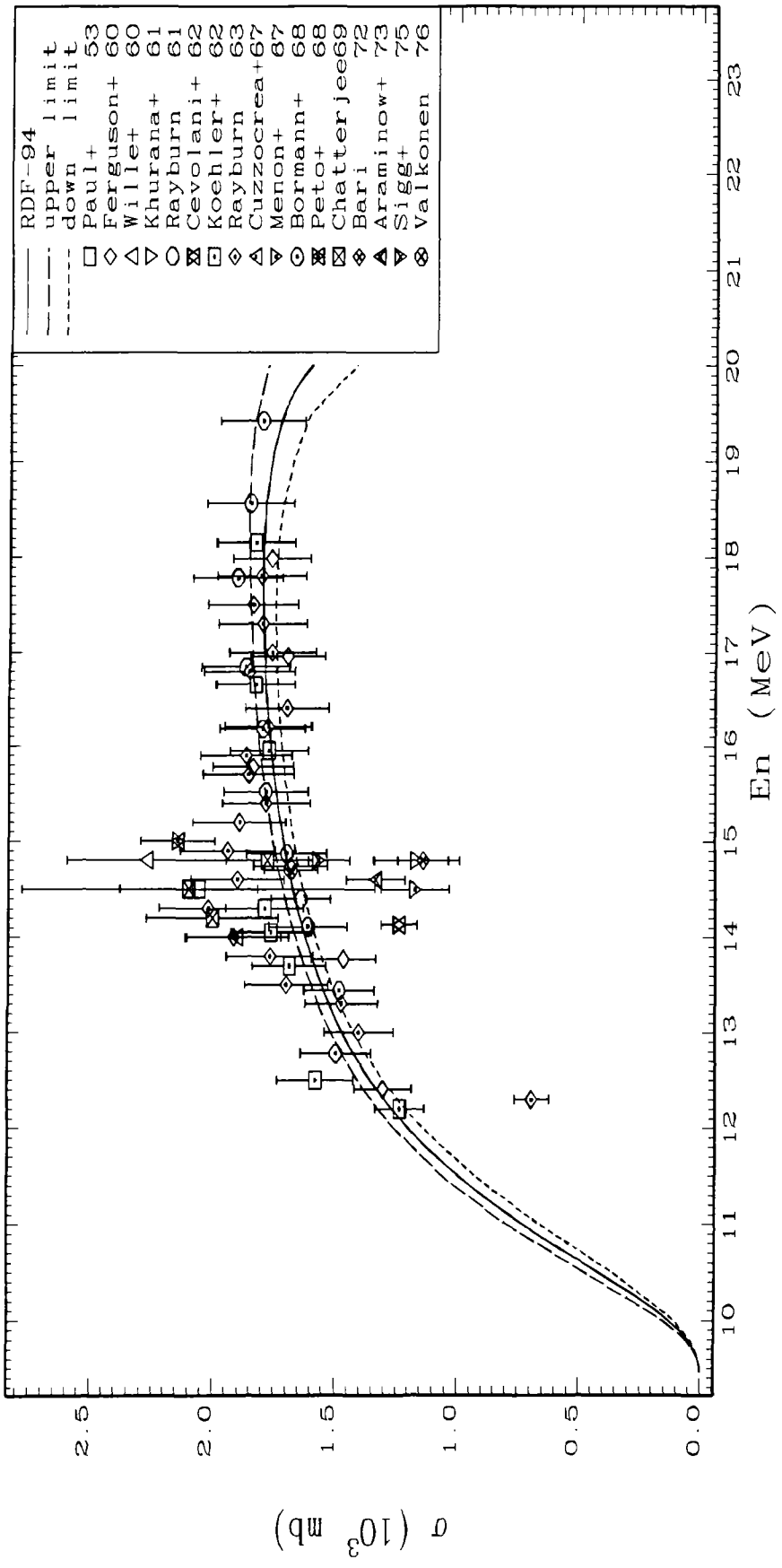

Fig. 1 Excitation function for the Pr141(n,2n)Pr140 reaction from present evaluation. Dashed lines are the upper and down limits of 1σ uncertainties.

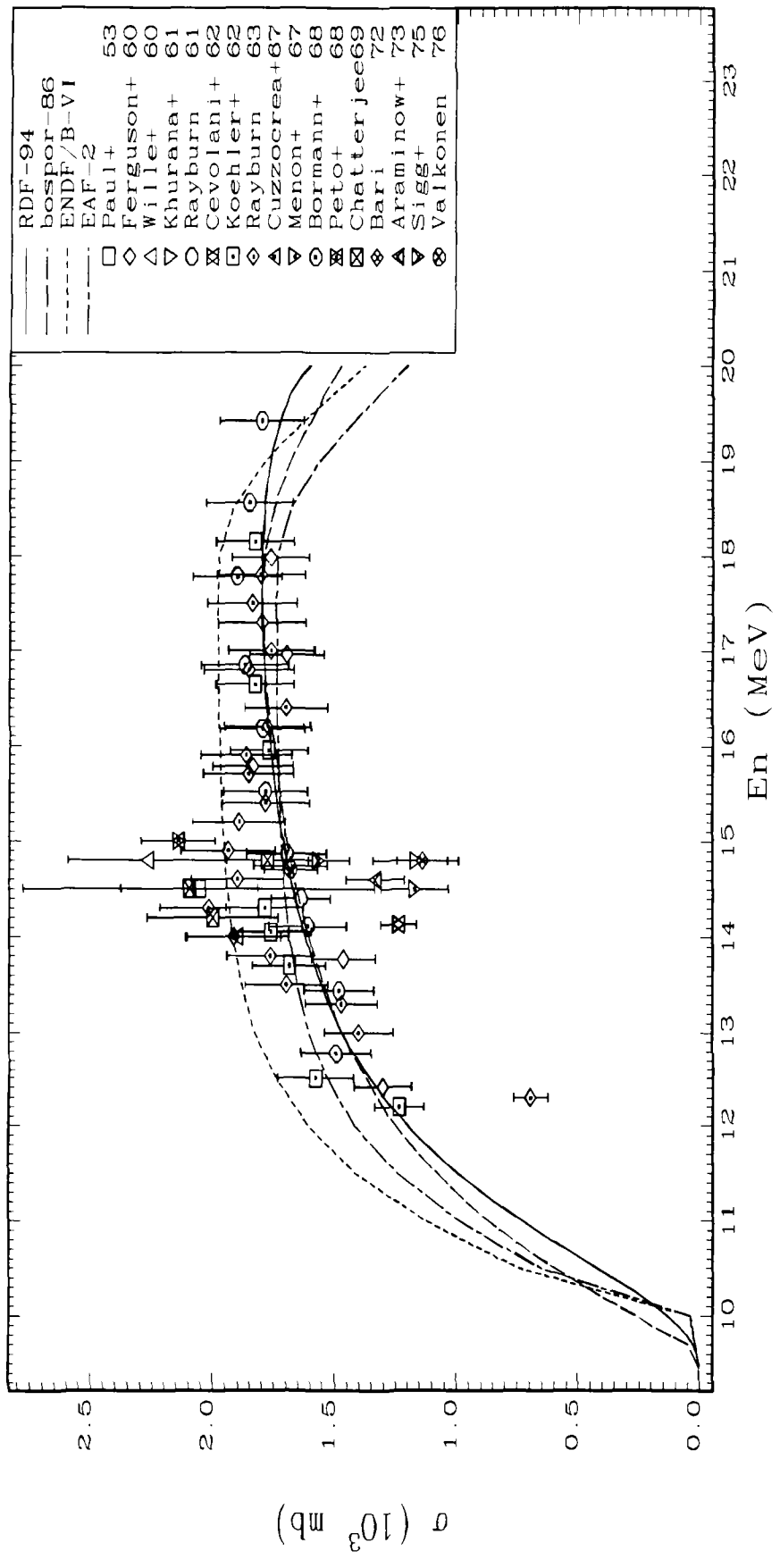

Fig. 2 Evaluated excitation function for the Pr141(n,2n)Pr140 reaction in comparison with experimental data and evaluated data from other libraries.

Nuclear Data Section
International Atomic Energy Agency
P.O. Box 100
A-1400 Vienna
Austria

e-mail, INTERNET: SERVICES@IAEAND.IAEA.OR.AT
e-mail, BITNET: RNDS@IAEA1
fax: (43-1) 20607
cable: INATOM VIENNA
telex: 1-12645 atom a
telephone: (43-1) 2060-21710

online: TELNET or FTP: IAEAND.IAEA.OR.AT
username: IAEANDS for interactive Nuclear Data Information System
username: NDSOPEN for FTP file transfer